The S1 domains of *Escherichia coli* mRNA degradation.

by Robert Edward Edge

Hon. B.Sc., Simon Fraser University, 2000

A THESIS SUBMITTED IN PARTIAL FULFILLMENT OF THE REQUIREMENTS

FOR THE DEGREE OF MASTERS OF SCIENCE

in

THE FACULTY OF GRADUATE STUDIES

Department of Biochemistry and Molecular Biology

We accept this thesis as conforming to the required standard

THE UNIVERSITY OF BRITISH COLUMBIA

December, 2003

Library Authorization

In presenting this thesis in partial fulfillment of the requirements for an advanced degree at the University of British Columbia, I agree that the Library shall make it freely available for reference and study. I further agree that permission for extensive copying of this thesis for scholarly purposes may be granted by the head of my department or by his or her representatives. It is understood that copying or publication of this thesis for financial gain shall not be allowed without my written permission.

Robert Edward Edge

Name of Author *(please print)*

18/12/2003

Date (dd/mm/yyyy)

Title of Thesis: The S1 domains of Escherichia coli mRNA degradation

Degree: Master of Science   Year: 2003

Department of   Biochemistry and Molecular Biology
The University of British Columbia
Vancouver, BC   Canada

Abstract

The S1 domain is a recurring theme in the enzymes of mRNA decay in *Escherichia coli*, occurring in polynucleotide phosphorylase (PNPase), ribonuclease II (RNase II), ribonuclease E (RNase E) and ribonuclease G (RNase G). This thesis focuses on the function of the S1 domain of PNPase and RNase E. In the former, the hypothesis examined was that the domain provides an RNA -substrate contact that imparts processive phosphorylysis to the enzyme. Results show that PNPase lacking this domain still possesses catalytic activity, although at an extremely reduced rate, but appears to retain processive phosphorylysis of RNA substrates. In addition, the isolated PNPase domain has a K_d for RNA that is very high, suggesting that this domain may not play a role in the interactions between PNPase and its substrate. The S1 domain of RNase E was studied as an isolated domain. NMR experiments conducted by Dr. Mario Schubert revealed the solution structure of this isolated domain as well as potential dimerization contacts and identified residues implicated in nucleic acid interaction. Crosslinking data confirmed the dimerization of this domain. CD spectroscopy showed that a classical temperature -sensitive mutation in this domain alters its structure. The work on the RNase E S1 domain also tested the hypothesis that the domain confers the preference of RNase E for monophosphorylated substrates. The data suggest that this domain indeed binds to RNA (K_d 2 μM to 5 μM); however, it displays no increased affinity for differentially phosphorylated RNAs or detectable sequence specificity.

Table of contents

List of Figures

List of Abbreviations

5' UTR	5' untranslated region
BR10	sequence cleaved by RNase E
CD	circular dichroism
Csp	cold shock protein
DEPC	diethyl pyrocarbonate
DNase	deoxyribonucleic acid nuclease
DTT	dithiothreitol
EDTA	ethylenediamine tetraacetic acid
FPLC	fine performance liquid chromatography
g	gravity
His-tagged	hexahistidine tagged
IPTG	isopropyl-β-D-thiogalactopyranoside
K_d	dissociation constant
KH	K-homology domain
LB	Luria-Bertani Broth
mRNA	messenger RNA
NMR	nuclear magnetic resonance
NOE	nuclear Overhauser effect
ob-fold	oligosaccharide/oligonucleotide binding fold
PBS	phosphate buffered saline
PMSF	phenylmethylsulfonyl fluoride
PNPase	polynucleotide phosphorylase
psi	pounds per square inch
RNase	ribonucleic acid nuclease

rne-1	*rne* containing the mutation G66S
SDS	sodium dodecyl sulphate
SDS-PAGE	SDS polyacrylamide gel electrophoresis
TBE	tris-boric acid-sodium EDTA
T_m	midpoint unfolding temperature
UV	ultraviolet
v/v	volume/volume

1 Introduction

Ribonucleic acid (RNA) is one of the most fundamental and important constituents of the living cell. RNA is central to the process of gene expression and assumes such diverse forms as messenger RNA (mRNA), transfer RNA (tRNA), and ribosomal RNA (rRNA) to enable the conversion of the cell's genetic information to enzymes and structural proteins. Therefore, an essential part of understanding gene expression mechanisms involves a thorough knowledge of RNA metabolism and structure. Transcription is one important aspect of RNA metabolism, but is beyond the scope of this thesis. The focus of this work is mRNA turnover, another important aspect of RNA metabolism.

1.1 mRNA degradation in E.coli

The quantity of a particular protein produced in the cell is a direct result of the concentration of the corresponding mRNA and its translational efficiency. The size of a particular mRNA pool, in turn, is a function of the transcriptional activity of the gene and the lifetime of the specific transcript in the cytoplasm. While it has long been known that mRNAs in the cytoplasm are unstable due to the presence of ribonuclease activity, Apirion first proposed a mechanism for the degradation of bacterial mRNAs in 1973 [1]. This was a paradigm shift from the view of mRNA degradation as a passive recycling of ribonucleotides to a complex mechanism of endoribonuclease and exoribonuclease activities that plays an active role in gene expression.

It is now evident, 30 years later, that different mRNA species have half-lives ranging from less than 2 min to greater than 15 min in *Escherichia coli* (*E. coli*), the organism for which the most data on mRNA degradation exists (for a review see Coburn

1

and Mackie [2]). The active turnover of mRNA enables this model bacterium to adapt to environmental changes and to increase the effectiveness of negative transcriptional regulatory signals. Active turnover of mRNA also enhances energy conservation in the cell. While less than 5% of RNA in the cell is mRNA, it makes up 60% of newly transcribed RNA; thus, the recycling of ribonucleotides through active turnover is critical for efficiency [3]. It has also been shown that mRNA decay mechanisms allow for the differential expression of polycistronic transcripts [4]. To add to the complexity of prokaryotic mRNA degradation, small antisense RNAs have recently been discovered to play a role in selective mRNA decay [5]. Moreover, the enzymatic machinery of mRNA decay includes a multienzyme protein complex dubbed the degradosome [6] as well as discrete ribonucleases. The complexity of mRNA degradation pathways indicates the importance of this process for control of protein expression.

1.1.2 Mechanisms and Models of mRNA decay

A modern model for mRNA degradation is presented in Figure 1, adapted and paraphrased from Coburn and Mackie [2]. This illustrates the coordination of exonucleases and endonucleases and the involvement of the degradosome. The pathway begins with a typical translationally active transcript as a 5' -triphosphorylated mRNA containing 3' -terminal secondary structure. The initial step is an endonucleolytic cleavage catalyzed by RNase E leaving a 5' - fragment containing a 3' – OH which, if unstructured, is subjected to the 3' - 5' exonuclease activity of PNPase and/or RNase II. These enzymes degrade such fragments to short limit oligonucleotides which are subsequently degraded by oligoribonuclease [7]. The products of the initial cleavage by RNase E are usually no longer functional as mRNAs and are left with a 5' - monophosphorylated end. RNase E exhibits increased activity towards 5' -

2
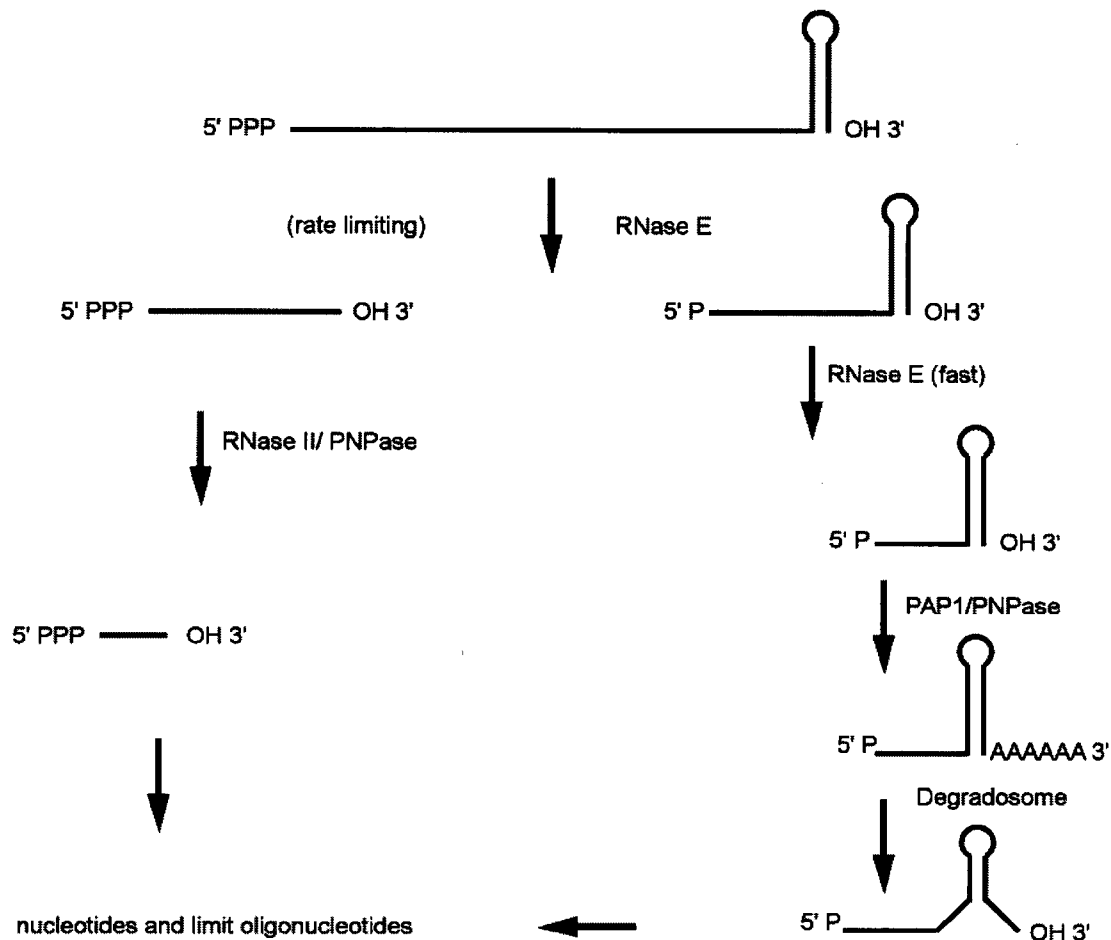
Figure 1: Model of mRNA decay in *E.coli of* a typical transcript containing a 5'
triphosphate and 3' -terminal secondary structure. Degradation of the transcript starts
with a rate limiting endonuclease cleavage by RNase E. This cleavage leaves single
stranded RNA (left side of the diagram) that is subject to further degradation by the
single-strand-specific 3' to 5' exonucleases, PNPase and RNase II. These reactions
produce limit mononucleotides and oligonucleotides as products. The initial cleavage
by RNase E (right side of the diagram) produces a RNA molecule (5' -
monophosphorylated) that serves as a better substrate for RNase E. The terminal
secondary structure is resolved by the multienzyme degradosome containing RNase E,
PNPase and an ATP dependant DEAD-box helicase, RhlB. The helicase unwinds the
secondary structure and produces single-stranded RNA which is subjected to the 3' to
5' exonuclease activity of PNPase resulting in the production of limit oligonucleotides.

monophosphorylated RNAs so that subsequent endonucleolytic cleavages occur much faster than the initial cleavage and the RNA is rapidly degraded [8]. Since the both 3' - 5' exonucleases are specific for single-stranded RNA, fragments generated by RNase E cleavages that contain secondary structure are resistant to further degradation. These fragments are can be degraded through the action of the multienzyme complex known as the degradosome [9]. This complex spatially coordinates the activity of RNase E, PNPase and RhlB, an ATP-dependent DEAD-box RNA helicase [10]. The RNA helicase is able to unwind RNA secondary structure in a reaction coupled to ATP hydrolysis that leaves unstructured single -stranded RNA as a substrate for phosphorolysis by PNPase. This mechanism provides many opportunities for differential stabilization of transcripts such as through secondary structure content and location and the accessibility of the 5' -end of the mRNA.

1.1.2 Enzymes of mRNA decay in E.coli

There are least 15 different RNases in *E.coli* evenly divided among endoribonucleases and exoribonucleases. Endoribonucleases hydrolyze phosphodiester bonds within an RNA polymer while exoribonucleases cleave phosphodiester bonds at the ends. Most of the exoribonucleases are not physiologically significant in mRNA degradation but instead process the stable tRNA and rRNA of the cell. These include RNase PH, RNase D, RNase BN (tRNA specific), RNase T and RNase R (rRNA specific). A very abundant periplasmic RNase of *E.coli* is RNase I, which may at most has a passive role in mRNA degradation. RNase H and RNase HI are involved in degradation of RNA primers following DNA replication. The only double strand-specific RNase is RNase III, the gene for which is dispensable for viability [11]. While there is great diversity of ribonucleases with specific substrates in *E.coli* only

RNase E (section 1.2.1), PNPase (section 1.2.2) and RNase II play a general role in mRNA degradation. RNase E and PNPase will be the primary topic of following sections.

1.2 ob-folds

A common feature of some key enzymes of RNA processing and decay is the presence of an S1 domain. The alignment in figure 2 indicates the position of an S1 domain in the N terminal region of RNase E and RNase G and in the C terminal region of PNPase and RNase II. The S1 domain is named after ribosomal protein S1, the protein in which it was initially characterized, and is a subclass of the ob-fold domains.

The ob-fold domain is a compact structural motif found in all three kingdoms and is frequently used for nucleic acid recognition (for reviews see [12-14]). The domain was first characterized by Murzin who named the ob-fold for oligonucleotide/ oligosaccharide-binding fold and after O.B. Ptitsyn [15]. These folds are grouped by topology and structure without significant sequence similarity. The domain consists of a five stranded antiparallel β-barrel ranging between 70 to 150 amino acids. This variability is largely a result of differences in variable loop structures between the conserved region of β-sheets. The conserved fold is arranged in a 1-2-3-5-4-1 β-sheet topology that is described as a Greek key motif. The most variable region occurs between β sheets 3 and 4 and is often composed of an alpha helix which packs against the bottom of the barrel effectively 'closing' the barrel. The conserved binding face has β strands 2 and 3 at its center and is bounded by the loops between the sheets. There are exceptions to these generalizations and there are cases where the ob-fold interacts with different macromolecules. This domain is utilized by different proteins to bind RNA, ssDNA, oligosaccharides or proteins. It can even form the catalytic site of some

5
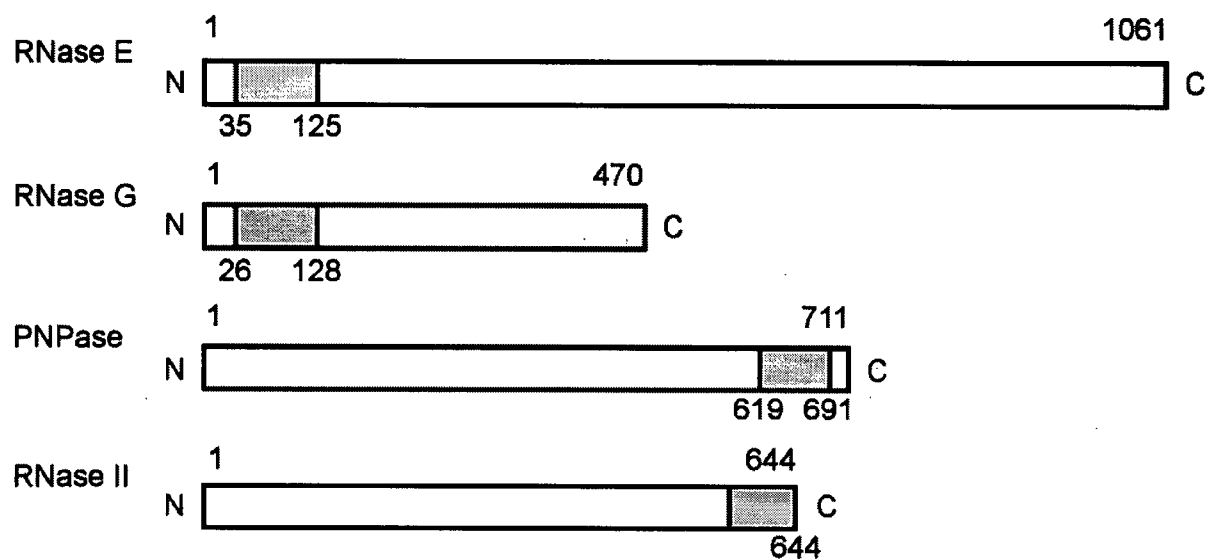
Figure 2: The S1 domains of enzymes of *E.coli* mRNA degradation. Each ribonuclease depicted is labelled with N and C terminal amino acid numbers. Grey boxes with amino acid numbers indicate the placement of the S1 domain of the enzyme. RNase E and RNase G, both endonucleases, have an S1 domain located near their N terminus while the exoribonucleases, PNPase and RNase II, have an S1 domain near their C terminus.

inorganic pyrophosphatases [13]. Generally these domains do not show any binding preference for nucleic acid sequence. In the majority of ob-fold proteins complexed with oligonucleotides, the bases of the nucleotide are in close contact with the protein while the phosphodiester bonds are mostly exposed to solvent. Nucleotides interact primarily via stacking interactions with aromatic amino acid side chains and interactions with hydrophobic aliphatic side chains of polar amino acids such as lysine and arginine. The *E.coli* ob-fold protein, CspB, been mutagenized to confirm the importance of basic and aromatic side chains in RNA binding [16].

1.2.1 RNase E

RNase E is an essential endoribonuclease of 1061 amino acids that is widely believed to be the principle RNase for the initiation of mRNA decay [17]. The data, however, are not completely unambiguous as, for example, most oligoribonucleotides isolated from *E.coli* contain 5' OH termini instead of the 5' -phosphomonoesters that would be produced from an RNase E cleavage [18]. What is of interest to this study is the function and specificity of RNase E, its domain and quaternary structure, and the involvement and interactions of this enzyme in the degradosome.

While the first identified function of this enzyme was the processing of 9S rRNA into pre-5S rRNA by two specific cleavage events [19], it has become clear this essential enzyme has many functions in *E.coli*. Additionally it has been demonstrated to be involved in the processing of the 5' -end of 16S rRNA [20], the maturation of the RNA subunit of RNase P [21], the degradation of RNA I, the antisense regulator of colE1 plasmid replication [22, 23], the processing of most if not all tRNAs [24-26], the degradation of many mRNAs including *trxA* (thioredoxin), *ssb* (single-stranded-DNA-binding protein), *uvrD* (DNA helicase II), *cat* (chloramphenicol acetyltransferase), *nusA*

7

(N utilization substance), *pnp* (polynucleotide phosphorylase) [27], *rpsT* [28-30], *rpsO* [31, 32], *malEFG*, *trp* operon, *his* operon, and total pulse labelled RNA [27, 33].

It has become clear from studies of RNase E substrates that the enzyme is single-stranded RNA-specific yet has a poorly defined consensus cleavage sequence [34]. The regulatory RNA, RNA I, contains a cleavage site that has been used extensively to model a consensus sequence and has been used as the basis for determination of various substrate sequence requirements of the enzyme [34-36]. Enzyme activity has also been demonstrated to require a 5'-unpaired residue. Also relevant to this study is the increased cleavage of 5'-monophosphorylated substrates over substrates that have a 5'-triphosphosphorylated end. RNase E is, therefore, said to exhibit 5'-end dependence [8]. This has lead to the hypothesis that this enzyme must contain a phosphate-binding pocket that preferentially binds monophosphorylated RNA thus accounting for its enhanced RNase E activity on these substrates.

The catalytic mechanism for RNase E is unknown. It is hypothesized, however, that the enzyme uses a two-metal-ion mechanism [37] as catalysis requires the presence of a divalent metal ion Mg^{++} or Mn^{++} [38]. Analysis of the amino acid sequence of RNase E reveals three distinct domains [39]. The N-terminal 500 amino acids encode the catalytic activity of the enzyme and are required for cell viability [40]. This domain is followed by an arginine and proline-rich domain (amino acids 567-684) demonstrated to have RNA binding properties *in vitro* [40-42]. This RNA binding domain (RBD) has been further delineated to residues 608-622, RRKPRQNNRRDRNER [2]. A similar motif is also found in the HIV-1 proteins Tat and Rev [43]. While this domain may have interesting implications for RNase E catalysis, including the recognition of cryptic cleavage sites [44], it is located in a region dispensible for catalysis [44, 45]. The C-

8

terminal domain (amino acids 734-1061) of RNase E is required for protein-protein interactions stabilizing the multienzyme complex known as the degradosome [46, 47]. Proteins shown to be a part of the degradosome and therefore interacting directly with this domain include PNPase, RhIB and enolase [48, 49]. The C-terminal domain is dispensable for catalytic activity, is not required for cell viability [50] and is not well conserved among prokaryotes, unlike the highly conserved N-terminal region of RNase E [51]. Nonetheless, it has been demonstrated that *E.coli* mutants containing this domain are more competitive in continuous culture than strains lacking the C-terminal domain [52].

The intracellular concentration of RNase E is regulated by an autoregulation mechanism. The *rne* transcript encoding RNase E is a substrate of its own product [53]. This autoregulation is mediated through a cleavage of the 5' -UTR of the *rne* mRNA [45, 54]. It also is through this mechanism that the *rne* transcript is stabilized in response to polyadenylation [55]. RNase E autoregulation requires the degradosome [55] and, therefore, the C -terminal region of RNase E [33, 56, 57].

Within the highly conserved N-terminal region from amino acids 35 - 125 is the putative RNA binding domain [58], an S1 domain, a member of the ob-fold domains. The two classical temperature-sensitive mutant loci, *ams*-1 (G66S) and *rne*-3071 (L68F), map to this domain [59, 60]. These mutations inhibit cell growth at non-permissive temperature. The more severe of these mutations, *ams*-1/*rne*-1, completely renders the enzyme inactive at 37°C *in vitro* [28](GA Mackie unpublished). These mutations highlight the importance of the correct folding of the S1 domain of RNase E for activity.

The only previous study of the S1 domain of RNase E modeled its three dimensional structure based on the structure of the PNPase S1 domain [58]. This enabled the engineering of mutations that were hypothesized to interact with RNA. Residues that were mutated in the study included aromatic and basic residues that were solvent-exposed in the model. The aromatic residues were hypothesized to provide base stacking interactions, while basic residues were hypothesized to provide ionic interactions with the phosphate backbone of the RNA ligand [61]. It was found that residues affecting RNA cleavage also affected autoregulation and mapped to one surface. Mutations that affected autoregulation alone and not *in vitro* catalysis mapped to a region slightly separated on the structural model from this first class of mutants [61]. The second region is not the typical surface of ob-folds that interacts with oligonucleotides. These mutations led the authors to hypothesize that this second class of mutations is located on a surface which recognizes specific RNAs such as the *rne* mRNA 5' -UTR. Alternatively, residues in the second region could be involved in a protein-protein interaction. The superantigens, a toxic subclass of ob-folds that show recent evolutionary divergence, provide precedent for ob-fold domains interacting with proteins [13].

1.2.2 PNPase

E.coli Polynucleotide phosphorylase (PNPase) is a 711 amino acid product of the *pnp* gene [62, 63]. PNPase was originally discovered and described as a template-dependent RNA polymerase enzyme with a subsequent rich history, being involved in the determination of the genetic code and site-directed mutagenesis [64, 65]. The enzyme is not essential in *E.coli*; however, mutant strains display a cold-sensitive phenotype [66]. PNPase uses inorganic phosphate in a phosphorylytic reaction that has

an absolute requirement for magnesium ions (or other divalent ions), and yields nucleoside diphosphates as a product. While this phosphorylytic mechanism predominates *in vivo*, the reverse polymerization reaction also can be induced *in vitro* and constitutes much of the enzyme's early history [64]. Both the requirement for a divalent ion and the structure hint at a reaction mechanism based on two metal ions with phosphate as an attacking nucleophile [37, 67]; however, details of the mechanism of PNPase activity are unknown.

Apart from the cold -sensitive phenotype, a null mutant of PNPase shows a mild phenotype and is viable. It is thought that the hydrolytic enzyme RNase II can compensate in the absence of PNPase. In support of this hypothesis, RNase II accounts for 90% of 3' – 5' exoribonucleolytic activity in crude extracts of *E.coli* [3]. Moreover, a double mutant of RNase II and PNPase is inviable [68]. It has also been argued that the two phosphorylytic exoribonucleases of *E.coli*, PNPase and RNase PH, have an essential role in ribosome biogenesis [66]. The phosphorylytic enzymes may also have evolved for energy conservation as products of the reaction are higher energy ADP molecules while the hydrolytic mechanism of RNase II produces AMP.

The role of PNPase in mRNA decay is evident in the activity and regulation of the enzyme. In *E.coli* mRNAs targeted for degradation are often polyadenylated [69] and polyadenylated substrates stimulate PNPase activity [69, 70]. This may be because PNPase is single-strand specific [71], making poly (A) RNA an ideal substrate. In addition to increasing the activity of PNPase towards RNA substrates, increased levels of total poly A in the cell increase the cellular concentrations of both PNPase and RNase E through interference with their separate autoregulatory mechanisms [55]. Poly

(A) tracts may sequester these enzymes to polyadenylated transcripts thereby stabilizing their respective mRNAs.

PNPase mutant *E.coli* cultures show greatly decreased growth rate at low temperature in comparison to wildtype. Recently it has been shown PNPase has a complex role in cold growth adaptation in *E.coli* [72]. PNPase is classified as a cold shock protein (CSP) and selectively degrades other CSP mRNA species following a cold shock response [73]. During the cold shock response expression of PNPase increases through a loss of its autoregulatory mechanism [74]. Normally, PNPase autoregulates its own expression by degrading the 5' -end of the *pnp* mRNA following an initiating cleavage catalyzed by RNase III [75]. Unlike the autoregulatory mechanism of RNase E, PNPase autoregulation, while dependent on RNase III, is independent of the degradosome [55].

The domain structure of PNPase consists of two duplicated regions with varying homology to RNase PH and two putative RNA binding domains, KH and S1 [76] (Figure 3). The crystal structure of *Streptomyces antibioticus* PNPase has been solved as a tungstate derivative [77]. This structure reveals PNPase is a trimer, and in a sense the enzyme consists of a trimer of the two duplicated regions homologous to RNase PH. The two duplicated regions are the two core domains of the trimer in the x-ray crystal structure of PNPase. The trimer is arranged with central pore where the tungstate electron density is located, hinting that this is the location of the site of phosphate binding. The two RNA binding domains, while not ordered in the crystal structure of Symmons et al., are recognizable motifs based on sequence.

A KH domain is located between amino acids 557 - 591 in PNPase. The most strongly conserved motif in a KH sequence is a GKxG tetrapeptide and the structure

12
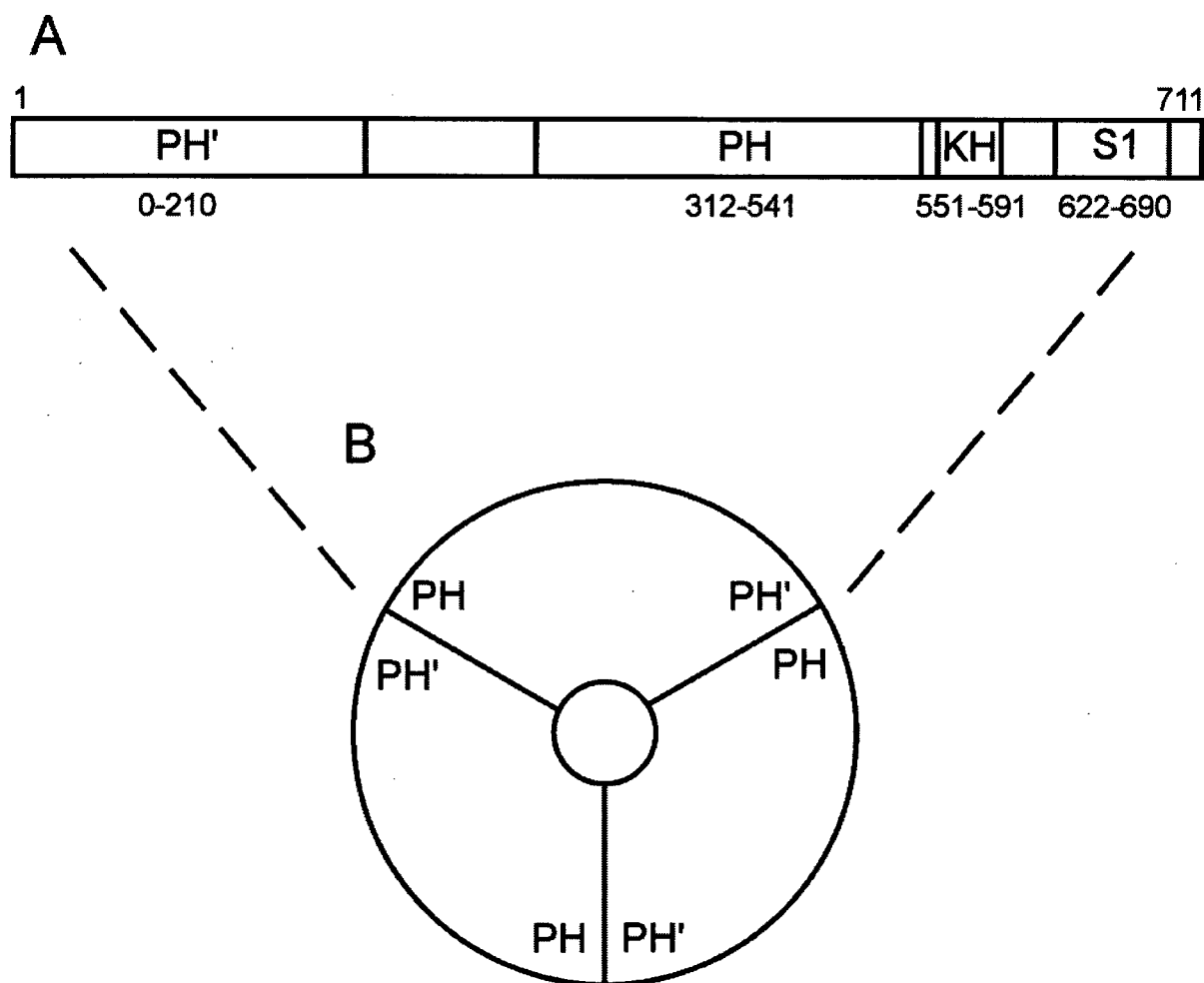
Figure 3: PNPase domain and quaternary structure. A. PNPase contains two domains with homology to RNase PH termed PH and PH' domains. B. These domains constitute a dimer of RNase PH-like domains in a trimer of PNPase. A central pore is evident in the PNPase trimer from the x-ray crystal structure of the *Streptomyces antibioticus* PNPase [59] and is indicated in the center of the PNPase trimer. The KH and S1 domains of PNPase were not localized in the crystal structure but are thought to be located out of the plane of the depicted structure.

consists of $\beta\alpha\alpha\beta\beta\alpha$ fold [78]. This domain has been shown previously to be an ssRNA binding domain by Northwestern blot [79]. Other examples of a KH domain include the KH domain of ribosomal protein S3 which can be cross-linked to ribosome-bound RNA [80], and *E.coli* NusA which has been shown to bind nascent mRNA [81]. The solution structure of the KH domain of human FMR1, which is associated with fragile X syndrome, has been solved and presents a hypothetical RNA binding surface [78]. A mammalian Nova KH domain has also been shown to have sequence specificity in binding RNA [82]. A detailed analysis of the interaction between any KH domain and RNA is, however, lacking. An analysis of PNPase engineered to lack the KH domain has shown that the mutant exhibits a slightly higher rate of phosphorylysis reaction, a lower rate of polymerization, but most significantly, a greatly reduced efficiency of autoregulation [83].

The S1 domain of PNPase is located between residues amino acids 619 and 691. The solution structure of this domain has been solved and contains a five stranded antiparallel β-barrel, typical of ob-fold domains [58] and exhibits strong structural homology to cold shock domains. Early kinetic studies of PNPase have established a hypothesis that processive catalysis by PNPase required the presence of distinct RNA binding sites that are separated by up to 20 – 40 nucleotides along the RNA substrate [84, 85]. These binding sites would allow the enzyme to maintain contact with the substrate during successive catalytic events and impart a processive mode of action to the enzyme. More recent mutational analysis indicates that PNPase lacking the S1 domain, similar to PNPase lacking the KH domain, is deficient in autoregulation [83].

An interesting property of the S1 domain of PNPase is its ability when overexpressed to suppress the phenotype of a quadruple deletion in the cspA family of

cold shock genes. The quadruple mutant in these cold shock proteins exhibits a cold-sensitive phenotype not unlike that of a PNPase mutant [86]. The CspA protein has a similar tertiary structure to the S1 domain of PNPase and is also classified as an ob-fold protein [87, 88]. It has been hypothesized that CspA is an RNA chaperone and maintains RNA in an unstructured conformation, thereby acting as a transcription antiterminator [89]. An NMR experiment in which CspA was titrated with a DNA ligand has revealed the interacting surface and residues involved in this interaction [87]. This suggests the possibility that the S1 domain of PNPase serves a function similar to CspA, but in the context of a 3' – 5' single-stranded exoribonuclease, and possesses a similar nucleic acid binding surface.

Ob-fold domains can also be involved in protein-protein interactions, as in the case of the bacterial superantigens where it serves as a dimer interface and to crosslink MHC-II molecules [13]. The C -terminal region of RNase E (residues 844 - 1045) is known to interact with PNPase in the degradosome, but which part of PNPase is responsible for this interaction has not definitively been shown. Preliminary data suggest that the S1 domain of PNPase may be responsible for this interaction with the C terminal region of RNase E (Miao, X., unpublished).

The role of the two RNA binding domains in PNPase remains unclear. It is possible that the KH and/or the S1 domains constitute the distinct RNA binding surfaces previously implied to be responsible for the processive nature of PNPase [84]. However, it is not known whether the effect on autoregulation is a result of loss of processivity or another function of these domains.

1.3 Focus of this study

The aim of this thesis is the examination of the role of the S1 domain in mRNA decay in *E.coli*. As described previously this domain is a recurring theme in enzymes involved in this process.

Two specific S1 domains will be examined in this thesis, one from RNase E and the other from PNPase. The S1 domain of RNase E was examined as an isolated domain. The solution structure of this fold was solved by nuclear magnetic resonance spectroscopy by Dr. Mario Schubert. This study attempts to examine the importance of specific residues and the specificity of the RNA binding capacity of this domain using the obtained structural data. The *rne*-1 mutation and some engineered mutations are also examined in this context. Evidence for the dimerization of this domain is also established. It has been suggested that the S1 domain of RNase E constitutes the hypothesized phosphate binding pocket responsible for the enzyme's activity towards monophosphorylated substrates. My data indicate that the S1 domain of RNase E alone can not account for this observation.

The role of S1 domain of PNPase in mRNA degradation is examined in terms of the function of the enzyme *in vitro* and *in vivo*. The phosphorolysis activity of this enzyme was examined in a construct lacking the S1 domain to test the hypothesis that this domain provides substrate contacts that account for its processive catalysis. Surprisingly the processivity of the reaction is maintained while catalytic activity is greatly reduced. In addition the function of this domain in the cold shock phenotype of a PNPase null mutant is examined.

16

2 Materials and Methods

2.1 Source of Reagents

All chemicals were purchased from commercial sources and were of reagent grade.

2.2 Bacterial Strains and culture techniques

Luria-Bertani broth (LB; 86 mM NaCl, 0.5% w/v yeast extract, 1% peptone) was used as a rich medium for culturing bacteria. Agar plates (LB supplemented with 1.5% agar) were used as a solid medium for isolation of single colonies. Plasmid selection on either medium was carried out by supplementation with one or more of ampicillin (100 μg/mL), kanamycin (30 μg/mL), or chloramphenicol (25 μg/mL). Manipulations of bacterial strains were performed aseptically as described (Sambrook, 1989).

2.3 Common Buffers

Lysis buffer: 25 mM Tris-HCl (pH 7.5), 0.1 mM EDTA, 2 mM DTT and 0.1 mM phenylmethylsulfonyl fluoride.

Buffer B: 25 mM Tris-HCl (pH 7.5), 0.1 mM EDTA, 2 mM DTT and 5% glycerol.

Anion exchange buffer: 50 mM Tris (pH 8.0), 50 mM NaCl and 0.5 mM DTT.

Talon buffer: 50 mM Tris-HCl (pH 8.0) and 500 mM NaCl.

Filter Assay Binding Buffer (FAB buffer) was made as a five-fold concentrated stock consisting of 100 mM sodium phosphate at pH 6.5 and 250 mM NaCl.

Buffer A: 20 mM Tris (pH 7.5), 1.5 mM DTT, 1.0 mM $MgCl_2$ and 20 mM KCl.

TBE buffer: 90 mM Tris, 90 mM Boric Acid, 2 mM EDTA.

Formamide Loading Buffer: 45 mM Tris, 45 mM Boric Acid, 1 mM EDTA, 90% deionized formamide, 0.02% each Xylene Cyanol and Bromophenol Blue.

Tricine solution: 10 mM Tricine (pH 7.9-8), 50 mM NaOAc and 5 mM EDTA.

SDS-sample buffer: 120 mM Tris-HCl pH 6.8, 3% sodium dodecylsulphate (SDS), 50 mM DTT, 10% glycerol, 0.1% bromophenol blue.

Laemmli buffer: 25 mM Tris-HCl, 192 mM glycine, 0.1% SDS.

Coomassie Brilliant Blue stain: 0.5 mg/mL Coomassie Brilliant Blue, 45% methanol, 10% acetic acid.

Destaining solution: 5% acetic acid, 5% ethanol.

Transfer buffer: 3 mM Na_2CO_3, 10 mM $NaHCO_3$, 20% methanol.

PTBN: 20 mM sodium phosphate (pH 7.0), 0.05% Tween, 0.1 mM bovine serum albumin, 0.85% NaCl, 1 mM NaN_3.

PBS: 137 mM NaCl, 2.7 mM KCl, 10 mM Na_2PO_4, 1.8 mM KH_2PO_4, adjusted to pH 7.4 with HCl.

Table 1: Table of strains

Strain	Genotype
BL21(DE3)	F⁻ *ompT hsdS$_B$*(r$_B$⁻, m$_B$⁻) *gal, dcm* λ(DE3)
DH5α	F⁻ *φdlacZΔM15 Δ(lacZYA -argF) U169 deoR recA1 endA1 hsdR17*(rK-, mK+) *phoA supE44* λ-*thi-1 gyrA96 relA1*
ENS134	F⁻ *ompT hsdS$_B$*(r$_B$⁻, m$_B$⁻) *gal, dcm* λ(DE3), pnp::Tn5

2.4 PCR and site-directed mutagenesis

Amplification of specific DNA sequences was achieved using the polymerase chain reaction (PCR) [90] in conjunction with a Perkin Elmer GeneAmp 2400 programmable thermocycler. PCR reactions typically consisted of up to 250 ng plasmid template or 1 μg genomic template DNA, 200 ng each of forward and reverse synthetic oligonucleotide primers, 0.2 mM each of the four deoxynucleotide triphosphates and 5 U of commercially available Taq DNA polymerase in the buffer supplied by the manufacturer, in 100 μL in thin walled polypropylene tubes.

Site-directed mutagenesis was achieved using a commercially available DNA polymerase with 3' to 5' proof-reading activity in a PCR reaction using the manufacturer's instructions as a guide (Stratagene Quick-Change kit). Synthetic oligonucleotide primers contained sequences that spanned the desired mutation and are listed in Table 2. The products of this reaction were treated with Dpn1 to digest the native dsDNA template. The remaining product was used to transform commercially competent DH5α (Invitrogen) to propagate the resultant plasmid for sequencing and transformation.

2.5 Other molecular biological methods

Well established molecular biological procedures such as restriction endonuclease digestion, DNA ligation, plasmid transformation, plasmid extraction, and gel electrophoresis were performed as described in Sambrook (1989) unless otherwise noted.

Table 2: Table of primers

Primer	Sequence	Mutant generated
RE16-M1	gaaatcgaagtgggccgcgtcgttgagaaagtgaccgattacc	PNPase ΔS1
RE16-M2	ggtaatcggtcactttctcaacgacgcggcccacttcgatttc	PNPase ΔS1
RE17-M1	cataccatcaagatcaacccggaagtgggccgcgtctacact	PNPase ΔKH
RE17-M2	agtgtagacgcggcccacttccgggttgatcttgatggtatg	PNPase ΔKH
RE23-M1	gttcagatcgataaagaagaggccggcaacaaaggcgcggc	R109A
RE23-M2	gccgcgcctttgttgccggcctcttctttatcgatctgaac	R109A
RE21-M1	gttgattacggcgctgaagctcacggtttcctcccactaaaag	F28A
RE21-M2	cttttagtgggaggaaaccgtgacgttcagcgccgtaatcaac	F28A
S1R35A-F	cggcgctgaagctcacggtttcctcc	R35A, E34D
S1R35A-R	ggaggaaaccgtgagcttcagcgccg	R35A, E34D

2.6 Enzyme Purifications

2.6.1 PNPase

PNPase was expressed in *E.coli* BL21 containing the plasmid pGC400 [91]. The bacteria were grown in 600 mL LB supplemented with ampicillin as selection for pGC400 at 37°C, until an OD_{600} of 0.4 – 0.6 was reached. IPTG was added to the cultures to 0.1 mM final concentration for induction of the expression of PNPase. Cultures were grown with aeration for an additional 4 hours at 37°C. Cells were harvested by centrifugation at 4, 000 x g for 10 min at 4°C. All subsequent steps were performed in a 4°C cold room. Cell pellets were resuspended in 5 mL of lysis buffer and

ruptured by passage through a French Pressure Cell at 10, 000 psi. The lysate, approximately 10 mL, was treated with 10 U DNase 1 for 15 min on ice. The lysate was then centrifuged at 30, 000 x g for 45 min and the supernatant was passed through a 0.22 μm syringe filter. The filtrate was applied to a FPLC column containing agarose supported heparin (4 cm x 2.5 cm), previously equilibrated with buffer B. The column was washed at 1 mL/min for 10 min before a gradient of NaCl from 0 – 1 M in buffer B over 2 hrs was used for elution. Fractions showing high UV absorbance at 280 nm were examined by SDS-PAGE. Those fractions containing PNPase, which eluted around 200 mM NaCl, were pooled and subjected to further chromatography. A SourceQ anion exchange column (4 cm x 2.0 cm), previously equilibrated with anion exchange buffer, was used on an FPLC at a flow rate of 1.0 mL/min. After the injection of the pooled fractions from the heparin column the column was pumped with anion exchange buffer for 10 min. A gradient of NaCl (50 mM-1 M in anion exchange buffer) was used to elute PNPase. Fractions containing PNPase were concentrated in a centrifugal filter with a 5 kDa cut off before being subjected to gel filtration on a 0.5 M cut-off column (48 cm x 2 cm) previously equilibrated with Buffer B containing 100 mM NaCl at a flow rate of 0.5 mL/min. The fractions containing PNPase as determined by SDS-PAGE were concentrated using a centrifugal filter and the resulting protein fraction was frozen in 50 μL aliquots at -80°C after the addition of glycerol to 5%.

2.6.2 S1 domain of RNase E

The RNase E S1 domain was expressed in *E.coli* BL21 containing the plasmid 'S1B-3', previously constructed by Mike Cook. The bacteria were grown in 300 mL LB supplemented with ampicillin at 37°C until early logarithmic phase. IPTG was added to the cultures 0.1 mM for induction of expression for 4 hours. The cells were then

harvested by centrifugation at 4, 000 x g for 10 min at 4°C and all subsequent steps were performed in a 4°C cold room. Cell pellets were suspended in 5 mL of talon buffer and ruptured by passage through a French Pressure Cell at 10, 000 psi. The lysate, approximately 15 mL, was treated with 10 U DNase I for 15 min on ice. The material was then centrifuged at 30, 000 x g for 45 min and the supernatant was diluted to 10 mL with talon buffer. This material was added to a 5 mL Co^{+2} chelating resin (Talon®, Clontech) in a gravity flow column and a flow rate of about 2 mL/min was achieved by hand pressure, applied with a 10 mL syringe. The column was previously equilibrated with Talon buffer. Step gradients of imidazole in talon buffer were applied to the column to elute weakly bound proteins initially and then to elute the His-tagged S1 domain in one fraction. The column was first washed with four column volumes of 5 mM imidazole followed by one column volume of 15 mM imidazole. Protein was then eluted with 1.6 column volumes of 50 mM imidazole. This was followed by a wash of 1.6 column volumes of 500 mM imidazole to remove any remaining bound proteins. Fractions were analysed by SDS-PAGE for purity. The His-tagged S1 domain which eluted in the 50 mM imidazole fraction was concentrated using a centrifugal filter with a molecular weight cut-off of 5 kDa to a volume of about 1 mL. This sample was then dialysed in the presence of 2 U of human thrombin for 16 hrs against 1 L of Talon buffer. To remove the thrombin, 200 µL of p-aminobenzamidine agarose beads were added to the sample and placed on a "neutator" shaking table at 4°C for 1hr. The samples were centrifuged at 16, 000 x g and the supernatant was diluted with Talon buffer to a volume of 5 mL. This sample was loaded on a pre-equilibrated Co+2 column and the flow-through was again collected at approximately 2 mL/min followed by a 5 mL wash with Talon buffer. This 10 mL flow through fraction was concentrated to 1 mL using a centrifugal filter with

a molecular weight cut-off of 5 kDa. This sample was dialysed for 16 hrs in 1 L of FAB buffer. Sterile glycerol to 5% v/v was added to the purified protein and the sample was stored at -80°C in aliquots. Purity and identity of the isolated domain was analysed by mass spectrometry as described in section 2.7.3.

Various methods were used in an attempt to remove contaminating RNase activities from the purified RNase E S1 domain. An entire preparation was applied to a reverse phase HPLC column in which a gradient of acetonitrile was used to elute the protein. Fractions of 4 mL were collected in 10 mL test tubes that had been DEPC treated, and the UV absorbance at 280 nm was monitored during the collection. Fractions showing the highest UV absorbance were lyophilized before being dissolved in FAB buffer.

2.6.3 RNase E

The preparation of the RNase E used in this thesis was done as described in a directed studies project.

2.7 Protein Analysis

2.7.1 Nuclear magnetic resonance (NMR) spectroscopy

Multidimensional NMR spectroscopy was performed by Dr. Mario Schubert and Dr. Lawrence McIntosh. These data were used by Dr. Mario Schubert to determine the solution structure of the RNase E S1 domain.

2.7.2 DNA titration

A solution of 1.4 mM RNase E S1 domain was titrated with increasing amounts of a 10 residue deoxyoligonucleotide, BR10, modeled after a characterized cleavage site in RNA I; 5' -ACAGTATTTG -3' [22, 34-36]. NMR spectroscopy was used to determine

residues whose chemical shifts are altered by interaction with DNA. Spectra were measured by NMR at 0, 0.2, 0.4, 0.6, 0.8, 1.0, 1.1, 1.4 and 1.6 molar ratios of DNA to protein. All data were collected and analyzed by Dr. Mario Schubert.

2.7.3 Mass spectrometry

50 μL samples of a 0.5 mg/mL solution of the protein of interest in FAB buffer were analyzed using electrospray mass spectrometry. The analysis was done by Dr. Shouming He at the U.B.C. Laboratory of Molecular Biophysics.

2.7.4 UV quantification

Quantification of purified protein preparations took advantage of their UV absorbance at 280 nm, using theoretical extinction coefficients as calculated by http://us.expasy.org/tools/protparam.html, based on amino acid sequence.

2.7.5 CD spectroscopy

All measurements were performed on solutions containing protein of at least a 0.25 mg/mL in a 400 μL, 0.2 mm quartz cuvette. Spectra were recorded on a Jasco J-810 spectropolarimeter, corrected for buffer background and reported in molar ellipticity (degrees.cm^2/decimole). Temperature variation experiments to determine an approximate T_m were done at a temperature change rate of 2°C/min with a data pitch of 0.5°C and at a wavelength of 225 nm. This wavelength was determined to be the most informative over the temperature range tested (10 - 80°C) for the wildtype RNase E S1 domain in FAB buffer. Wavelength scans were done at 10°C temperature intervals from 25°C to 75°C and scanned from 190 nm to 250 nm.

2.7.6 Sodium dodecylsulphate polyacrylamide gel electrophoresis (SDS-PAGE)

Equal volumes of sample and SDS-sample buffer were mixed and boiled at 95°C for 2 min. Samples were then loaded onto a 7.5 or 15% polyacrylamide gel (36:1 or 29:1 respectively) containing 0.1% SDS and separated using Laemmli buffer at 140-190 V. After the bromophenol blue had run off the gel, proteins were visualized by staining with Commasie Brillant Blue in acetic acid and methanol for 5 – 10 min with agitation before being destained with destaining solution for as long as overnight.

2.7.7 Western Blotting

Samples were initially separated by SDS-PAGE and then blotted to a nitrocellulose membrane at 250 mA for 2 hrs in Transfer buffer. These blots were then blocked in 15 mL PTBN for 1 hr with agitation at room temperature, before the PTBN was decanted and replenished with polyclonal primary antibody at an appropriate dilution (5, 000 - 10, 000 fold in PTBN) and again incubated for 1 hr with agitation at room temperature. Three separate washes with PBS for 5 min were followed by incubation of the secondary antibody, goat anti-rabbit polyclonal antibody conjugated to horse radish peroxidase, in 15 mL of PBS for 1 hr at room temperature. This blot was then washed three times for 5 min each with 15 mL PBS. The blot was then wetted with a peroxidase chemiluminescent substrate and exposed to film for 1 to 5 min.

2.7.8 Glutaraldehyde crosslinking

Reactions consisted of 45 µM total protein in FAB buffer. Samples of 50 µL were incubated at 37°C for 2 min in 0.01% glutaraldehyde. To quench the reaction 10 µL of 300 mM Tris-HCl pH 8.0 was added and placed on ice. To concentrate the sample for

analysis 40 µL of 17.5% trichloroacetic acid was added and the mixture left on ice for 30min. Samples were then centrifuged at 13, 000 rpm for 15 min at 4°C and the precipitate was washed twice with 200 µL 80% acetone. For SDS-PAGE analysis samples were dissolved in 10 µL of SDS loading buffer and denatured by boiling for 2 min at 95°C.

2.8 RNA substrates

2.8.1 Template preparation

All substrates used were previously designed, cloned and described in the Mackie lab. Substrates SL9 and SL9A were generated using the plasmid pTZ18U [92] linearized with BamH1 and Xba1 respectively. Linearized DNA was purified from undigested DNA by agarose gel electrophoresis followed by purification using a commercial gel purification kit (QIAGEN gel purification kit). The final product was dissolved in DEPC-treated sterile water.

2.8.2 In-vitro transcription

Transcription of internally labeled RNA, for use as substrates for endoribonuclease and exoribonuclease assays, was performed as described previously [93]. Essentially this reaction was catalyzed by T7 RNA polymerase (6 U/µL) using 0.6 µg of linear DNA template (see section 2.8.1). The reaction also included all 4 ribonucleotides with GTP, ATP, and UTP at 0.5 mM, CTP at 50 µM and α-^{32}P-CTP at 375 nM as a label. The reaction contained 0.8 U/µL of a commercially available porcine RNase inhibitor (RNasei). The reaction was incubated at 30°C for 2 hrs before being quenched with three reaction volumes of 10 mM EDTA and 2.6 M NH$_4$OAc.

Quantification took place by comparison of total ^{32}P radioactivity to total precipitatable ^{32}P in 2.5 µL samples. One sample was counted directly, the other after precipitation with 5% trichloroacetic acid (TCA) in the presence of 10 µg/mL BSA on ice for 15 min. The precipitated RNA was then filtered under vacuum, washed with 5% TCA, and the filter dried by washing with acetone. The remainder of the reaction was extracted twice with phenol/chloroform/isoamyl alcohol (25:24:1) (PCI) and then precipitated with 2.5 volumes of ethanol. The pellet was washed with 80% ethanol to remove salt. Based on calculated yields, the transcribed RNA was diluted to 0.2 µM for use in ribonuclease and binding assays.

2.8.3 Monophosphorylation of RNA

For substrates where it was desired to have a 5' monophosphorylated RNA product, RNA was prepared as in section 2.8.4 but the pellet was dissolved in 75 µL of Tricine solution. The RNA was passed through a commercially available size exclusion spin column (Amersham-Pharmacia, G-25 spin column) to remove unincorporated deoxynucleotides and short abortive transcripts. RNA is synthesized with a tri-phosphorylated 5' end; these phosphates were removed enzymatically by 150 U/mL calf intestinal phosphatase (Amersham Biosciences) in the supplied buffer. The phosphatase reaction was incubated at 37°C for 30 min before the enzyme was inactivated by continued incubation at 37°C in the presence of 0.1% SDS, 5 mM EDTA and 50 µg/mL proteinase K for 15 min. The protease treatment was stopped by diluting the reaction with one volume of 0.25% SDS and 300 mM sodium acetate. The digest was extracted twice with PCI and then precipitated with 2.5 volumes of 95% ethanol. The precipitated RNA was washed with 80% ethanol, and then dried at ambient temperature and pressure. The phosphorylation reaction was initiated by dissolving the

27

RNA pellet in DEPC-treated water and incubating the RNA for 35 min at 37°C in the presence of 10 mM Tris-acetate pH 7.9, 10 mM Mg-acetate, 50 mM K-acetate, 50 μM DTT, 500 μM ATP, 0.8 U/μL RNasin (RNase inhibitor, Amersham) and 0.3 U/μL polynucleotide kinase (PNK). This reaction was quenched by the addition of 2 volumes of 7 mM EDTA, 600 mM NH_4OAc and extracted once with PCI. The product was then precipitated overnight at -80°C after the addition of 2.5 volumes of ethanol. After centrifugation and decantation the pellet was dissolved in DEPC-treated H_2O, quantified by scintillation counting, and then further diluted in DEPC-treated H_2O to an estimated concentration of 0.2 μM. All transcripts were kept at -20°C in 50 μL aliquots.

2.8.4 End -labelling of homopolymer RNA

Homopolymeric RNA of an undefined length was obtained from Sigma chemical company. Each polymer was separately dissolved in 0.1 M Tris-HCl pH 7.0 and quantified assuming that 1 A_{260nm} unit is 40 μg/mL RNA and an average polymer length of 100 nucleotides to estimate the molarity. Each homopolymer was then dissolved to a concentration of 15 μM for use in an end-labelling reaction. The reaction consisted of about 30 pmol RNA, 10 mM Tris-acetate pH 7.9, 10 mM Mg-acetate, 50 mM K-acetate, 875 nM ATP, γ-^{32}P-ATP as a label and 0.5 U/μL polynucleotide kinase and was incubated for 35 min at 37°C. Following the incubation the reactions were chilled on ice and quenched with 160 mM NH_4-acetate, 8 mM EDTA and the reaction volume was increased to 50 μL with DEPC-treated water. All reactions were extracted once with chloroform/isoamyl alcohol (24:1), speed vacuumed to dryness, and resuspended in 40 μL DEPC-treated water. To rid the reaction of unincorporated nucleotides a G-25 sephadex spin column was used according to the manufacturer's instructions. The volume of the sample was increased to 150 μL and aliquots were frozen at -80°C.

2.8.5 Exoribonuclease assay

Internally ^{32}P labelled SL9A RNA was prepared as described in section 2.8.2. The assay mixture (32 μL) contained 0.8 pmol of RNA in Buffer A. Before addition of the enzyme this mixture was heated for 2 min at 50°C, then at 37°C for 10 min and finally placed on ice for at least 2 min. This heating regime was intended to ensure that the RNA refolded into the expected secondary structure. At time zero 8 μL enzyme was added in a 50 mM phosphate buffer pH 7.5. A zero time point was taken by immediately removing a 4 μL sample and mixing with 12 μL Formamide Loading Buffer. The assay continued at 30°C and 4 μL samples were removed at various time points, as in the zero timepoint, and mixed with 12 μL Formamide Loading Buffer. Following the assay portions of the 16 μL samples were separated on polyacrylamide gels containing 8 M Urea in TBE buffer.

2.8.6 Endonuclease Assay

Internally labelled 9S RNA substrate [93] was prepared as described in section 2.8.2. The assay mixture contained 5 mM Tris pH 7.5, 1 mM $MgCl_2$, 20 mM NH_4Cl, 50 μM DTT and 12 mM KCl along with 6.7 nM of the prepared labelled RNA. Before addition of the enzyme this mixture was heated for 2 min at 50°C, then at 37°C for 10 min and finally placed on ice for at least 2 min. This heating regime was intended to ensure that the RNA refolded into the expected secondary structure. At time zero 8 μL enzyme was added to the assay buffer above with glycerol resulting in a final glycerol concentration of 0.05%. A zero time point was taken by immediately taking a 4 μL sample and mixing with 12 μL Formamide Loading Buffer. The assay continued at 30°C and 4 μL samples were removed at various time points, as in the zero timepoint, and

mixed with 12 μL Formamide Loading Buffer. Following the assay portions of the 16 μL samples were separated on polyacrylamide gels containing 8 M Urea in TBE buffer.

2.9 Filter binding assay

The filter binding assay used in this study was adapted from an established double-filter method specifically for protein-nucleic acid interactions [94]. The assay utilized a 96 well dot blot apparatus in which samples were placed in separate wells on a 0.45 μm nitrocelllulose membrane overlaying a nylon membrane. Both membranes had previously been wetted in distilled water for 5 min. A central vacuum source was used to pull 50 μL of 1x FAB buffer through both membranes for equilibration. Samples were prepared on ice and contained 4 nM labelled RNA and various dilutions of protein in 1x FAB. These samples were added to each well and left at room temperature for 5 min. The vacuum was then again applied to the apparatus for 2 min before each well was washed with 100 μL FAB buffer at room temperature. The vacuum was continued for an additional 5 min before membranes were removed from the apparatus and allowed to dry. Membranes were exposed to a phosphoimager screen which was quantified using Image Quant software. To calculate the fraction of RNA that is bound at equilibrium for each well, the intensity of the signal on the nitrocellulose is divided by the sum of the signal from the nitrocellulose and the nylon membranes (ie. Bound/(Bound + Unbound) = Fraction Bound). Non-specific binding of the RNA or DNA to the nitrocellulose was found to be negligible and therefore not included in the calculation.

3 Results

3.1 RNase E S1 domain

3.1.1 Overview: nature of the problem/hypothesis

To investigate the function of the S1 domain of RNase E the domain was examined in isolation with a working hypothesis that this domain functions bind to substrate RNA molecules. It was also hypothesized that this domain provides the phosphate binding pocket that is responsible for the increased endonuclease activity of RNase E on monophosphorylated substrates relative to triphosphorylated substrates. This problem was first examined in a structural context to confirm sequence alignments that this domain is indeed an ob-fold. The capacity of this domain to bind RNA was also examined using a filter binding assay. In addition, mutants in the S1 domain, both engineered and a classical-temperature sensitive mutant, were examined for their structural and functional properties.

3.1.2 Expression and Purification

The DNA sequence of the *E.coli* RNase E S1 domain, encoding amino acids 35 - 125 of RNase E, was cloned into the BamH1 site of the plasmid vector pET15b (see Table 3). The vector, pET15b, contains a T7 polymerase promoter which allows for protein production in strains expressing T7 polymerase under *lac* operon control. The cloning work was done previously by Mike Cook and the plasmid named S1B-3. The protein was expressed and purified from BL21 as described in Materials and Methods (section 2.6.2).

Steps in the purification procedure were monitored by separating samples from intermediate steps in the procedure on an SDS-PAGE gel (see Materials and Methods,

section 2.7.6). Typical results are shown in Figure 4 for the wild type S1 domain of RNase E and Figure 5 for the *rne-1* G66S mutant. In Figure 4A and Figure 5A it can be seen that the majority of pure protein elutes at approximately 50 mM imidiazole. After the thrombin cleavage reaction most of the protein elutes in the Talon column flow through (Figure 4B lane 3 and Figure 5B lane 3). Both purification procedures show a mobility change after dialysis in the presence of thrombin confirming that the hexahistidine tag was cleaved. Samples of purified protein used in subsequent experiments are shown in Figure 4B Lane 4 for the wild type RNase E S1 domain and in Figure 5B Lane 5 for the *rne-1* G66S mutant. A protein contaminant of about 70kDa is visible in the final purified fraction of both preparations.

The ams-1 (also called *rne-1*) mutation is a temperature-sensitive mutation in RNase E that maps to amino acid 66 changing glycine to serine (G66S). This mutation renders cells inviable at the non-permissible temperature and RNase E catalytically inactive at $\geq 37°C$. The *rne-1* mutation was inserted into the S1B-3 construct using site-directed mutagenesis (see Materials and Methods, section 2.4) by Mike Cook. Since this temperature-sensitive mutation is responsible for abolishing RNase E activity both *in vivo* and *in vitro*, its effect was investigated in the context of the isolated domain.

3.1.3 CD Spectroscopy

The stability of the domain was examined using circular dichroism (Materials and Methods, section 2.7.5). This allowed an estimate of the melting temperature (T_m) of the domain, and a comparison to the *rne-1* domain. As the latter mutation is temperature-sensitive, an altered T_m was anticipated. It is apparent from the spectra, even at 25°C, that the *rne-1* mutant domain has a different absorbance profile than wild-type (see Figures 6 and 7). Moreover, both protein samples show altered spectra at 75°C

Figure 4: Purification of the S1 domain of RNase E. The S1 domain of RNase E was purified as described in Materials and Methods (section 2.6.2). Various fractions were separated on a 15% SDS-PAGE gel (see Materials and Methods section 2.7.6). A: Lane 1, Molecular size markers; the sizes of each marker are indicated to the left. Lane 2, the S30 fraction; Lane 3, Talon column flow through; Lane 4, 5mM imidazole wash; Lane 5, second 5mM imidazole wash; Lane 6, 15mM imidazole wash; Lane 7, 50mM imidazole wash; Lane 8, 500mM imidazole wash. Pooled fractions corresponding to Lane 7 were concentrated and dialysed overnight in the presence of thrombin as described in Materials and Methods (section 2.6.2). B: Lane 1, Molecular size markers; Lane 2, preparation before dialysis in the presence of thrombin; Lane 3, preparation after dialysis in the presence of thrombin; Lane 4, flow through; Lane 5, 500mM imidazole wash.
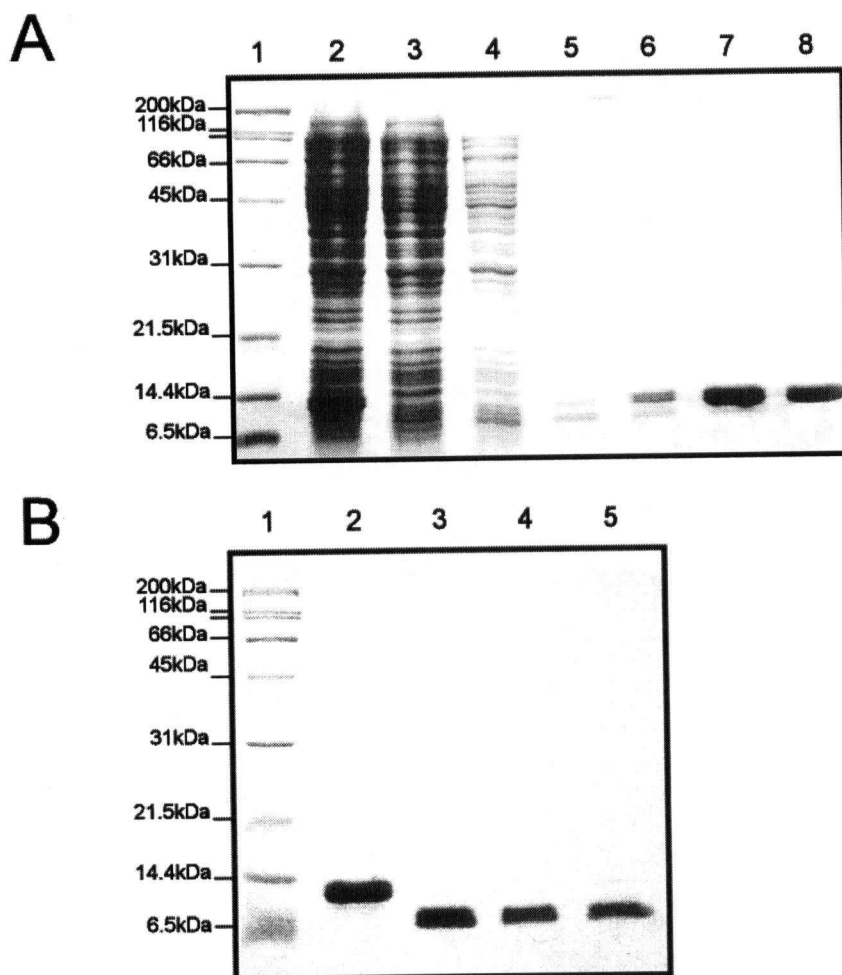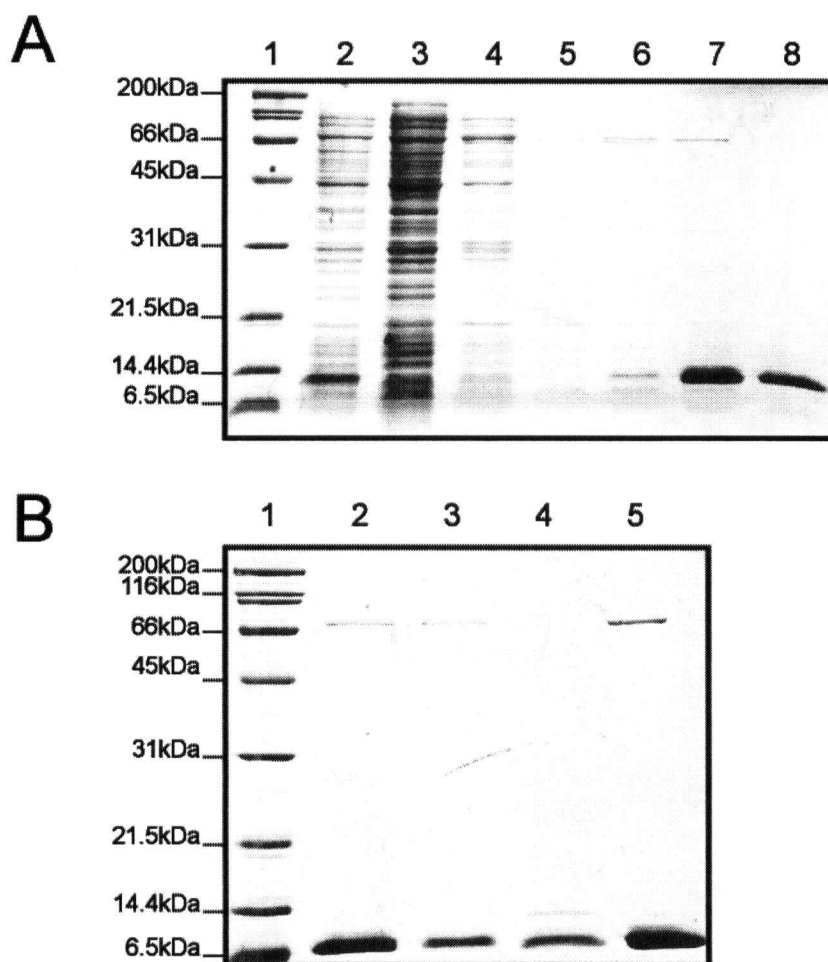
Figure 5: Purification of the rne-1 S1 domain of RNase E . The rne-1 S1 domain of RNase E was purified as described in Materials and Methods (section 2.6.2). Various fractions were separated on a 15% SDS-PAGE gel (see Materials and Methods section 2.7.6). A: Lane 1, Molecular size markers; the sizes of each marker are indicated to the left; Lane 2, the S30 fraction, Lane 3, Talon column flow-through of S30; Lane 4, 5mM imidazole wash; Lane 5, second 5mM imidazole wash; Lane 6, 15mM imidazole wash; Lane 7, 50mM imidazole wash; Lane 8, 500mM imidazole wash. Pooled fractions corresponding to Lane 7 were concentrated and dialysed overnight in the presence of thrombin as described in Materials and Methods (section 2.6.2). B: Lane 1, Molecular size markers; Lane 2, preparation after dialysis in the presence of thrombin; Lane 3, Talon column flow through; Lane 4, 500mM imidazole wash; Lane 5, flow-through after concentration.
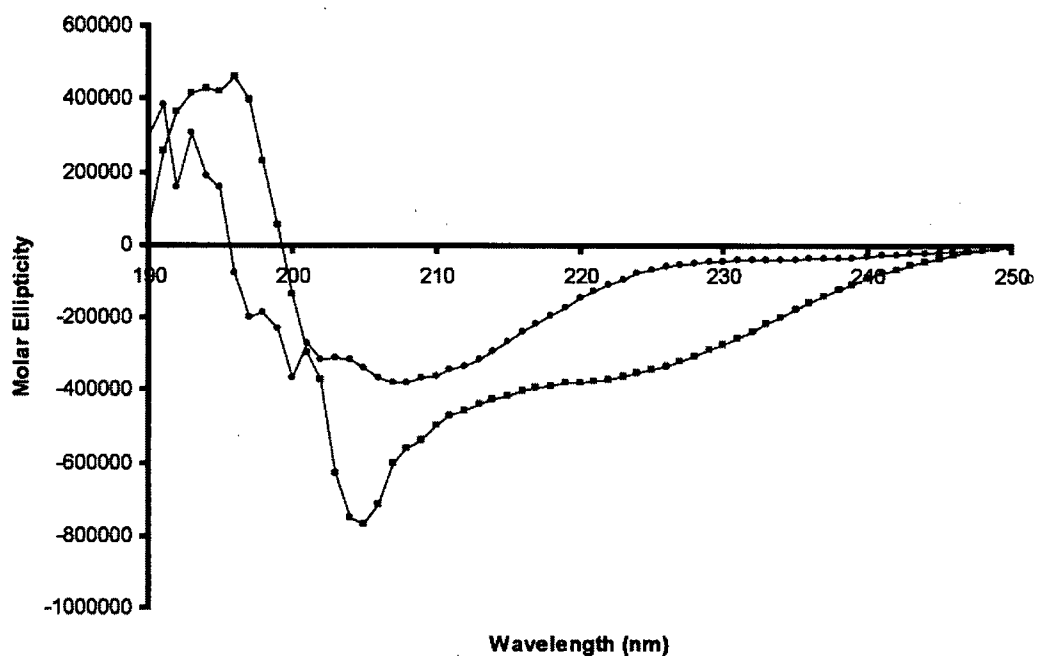
Figure 6: Circular Dichroism spectra of the RNase E S1 domain. Spectra were recorded on a Jasco J-810 spectropolarimeter with a protein concentration of 35 µM in FAB buffer. Each plotted spectrum is an average of 2 accumulations at the indicated temperature with a resolution of 0.5 $^{\circ}$C. Molar ellipticity is reported on the vertical axis in degrees.cm^2/decimole at 25 $^{\circ}$C (•) and at 75 $^{\circ}$C (∎) plotted against the incident wavelength.
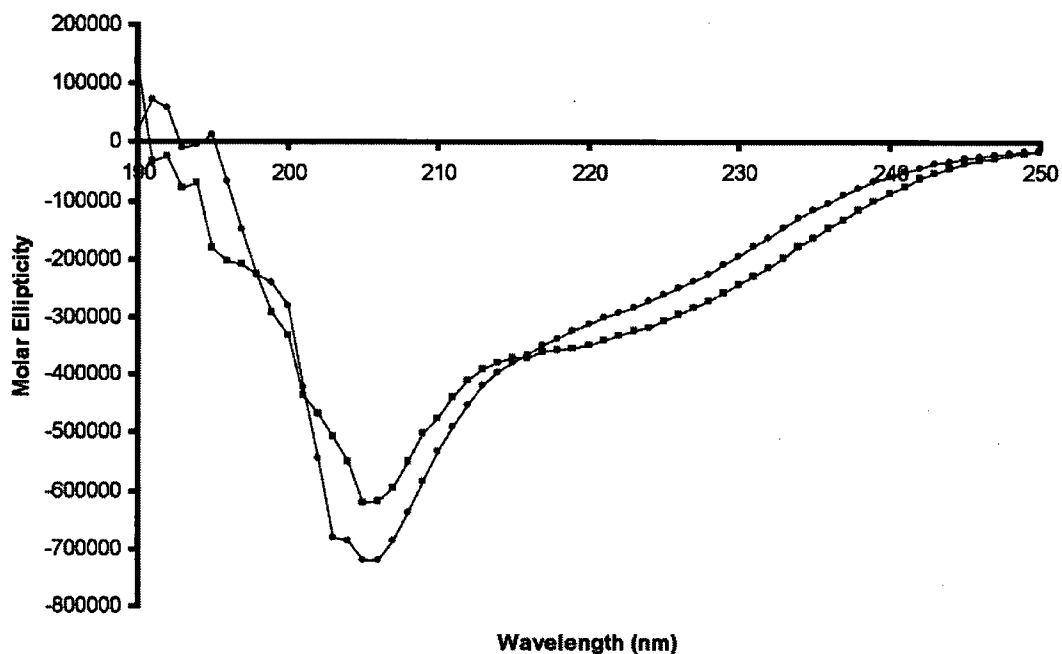
Figure 7: Circular Dichroism spectra of the RNase E S1 domain containing the *rne*-1 mutation. Spectra were recorded on a Jasco J-810 spectropolarimeter with a protein concentration of 35 µM in FAB buffer. Each plotted spectrum is an average of 2 accumulations at the indicated temperature with a resolution of 0.5 °C. Molar ellipticity is reported on the vertical axis in degrees.cm^2/decimole at 25 °C (•) and at 80 °C (■) plotted against the incident wavelength.

compared to 25°C. A CD melting curve was generated for both the wild type and *rne-1* domains using the molar ellipticity at 225nm as an indicator of secondary structure content. Examination of the resultant curves reveal an estimated T_m for the wild type domain of 50°C while the *rne-1* mutant has an estimated T_m at least 5°C lower (Figure 8). These melting curves also reveal that the structure of the *rne-1* mutant domain is much different than the wild type domain even at low temperatures. The data indicate that the *rne-1* mutation leaves this domain with less secondary structure at physiological temperatures. In addition, the structure is likely in equilibrium between a folded and unfolded state that favours the unfolded state to a greater extent than in the wild type domain.

3.1.4 Protein structural properties

Nuclear magnetic resonance (NMR) experiments required specific isotopic labelling of the protein. To achieve this, cells containing S1B-3 were grown in M9 media supplemented with appropriate isotopically labeled substrates. Labelling of the domain enabled use of multidimensional nuclear magnetic resonance (NMR) and resulted in a successful structure determination by Dr. Mario Schubert working with Dr. Lawrence McIntosh. The structure of this domain was confirmed as a classical ob-fold with 5 stranded anti-parallel β sheets (Figure 9). The β sheets are arranged in a Greek key topology with a 1-2-3-5-4-1 arrangement. The domain contains extended loops between sheets 3 and 4 that contain alpha helical content.

Unexpectedly, crystals formed during the storage of the protein sample used for NMR experiments. These crystals were found to diffract to resolution sufficient for structure determination. Additional protein samples were produced, were crystallized using the initial conditions, and were used by Dr. Mario Schubert and Dr. Paula Lario for
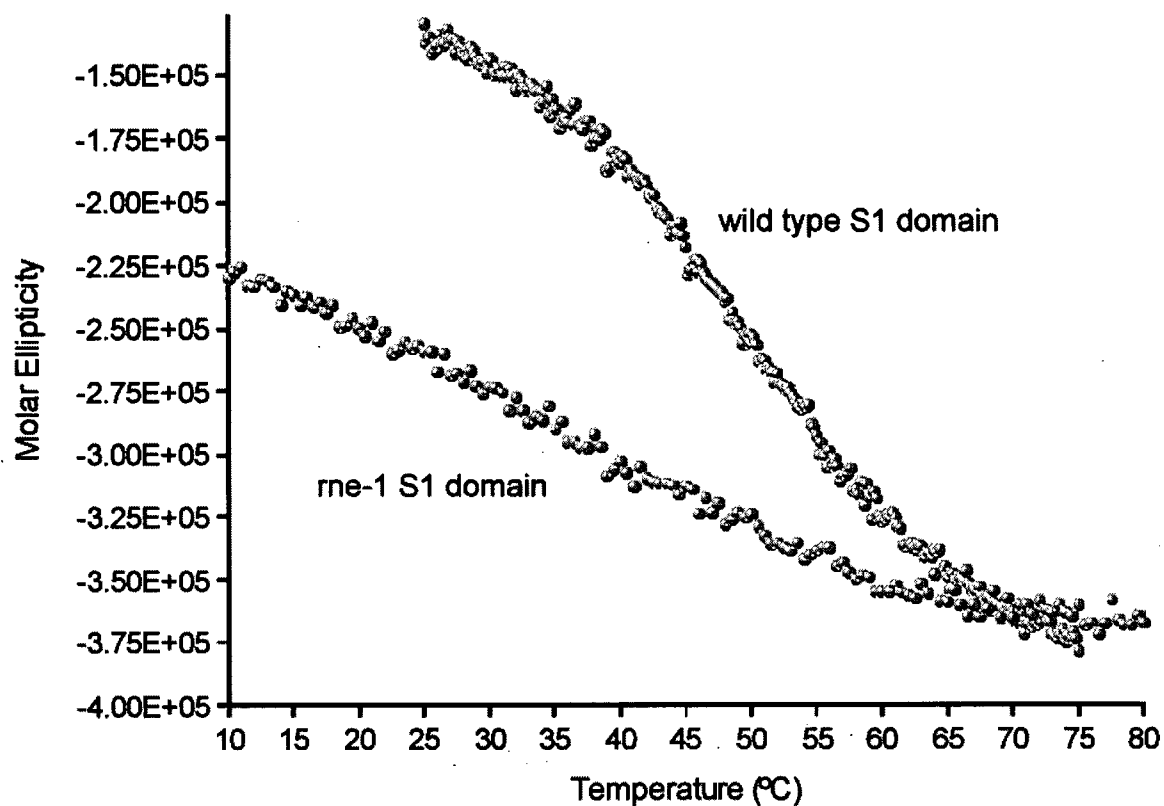
Figure 8: Thermal stability of S1 domains as measured by CD spectroscopy. Ellipticity of wild type and rne-1 RNase E S1 domains in pH 6.5 phosphate buffer, each at a concentration of 35 μM was measured at 225nm over the temperature range indicated (see Materials and Methods, section 2.7.5). Molar ellipticity is reported on the vertical axis in degrees.cm^2/decimole.
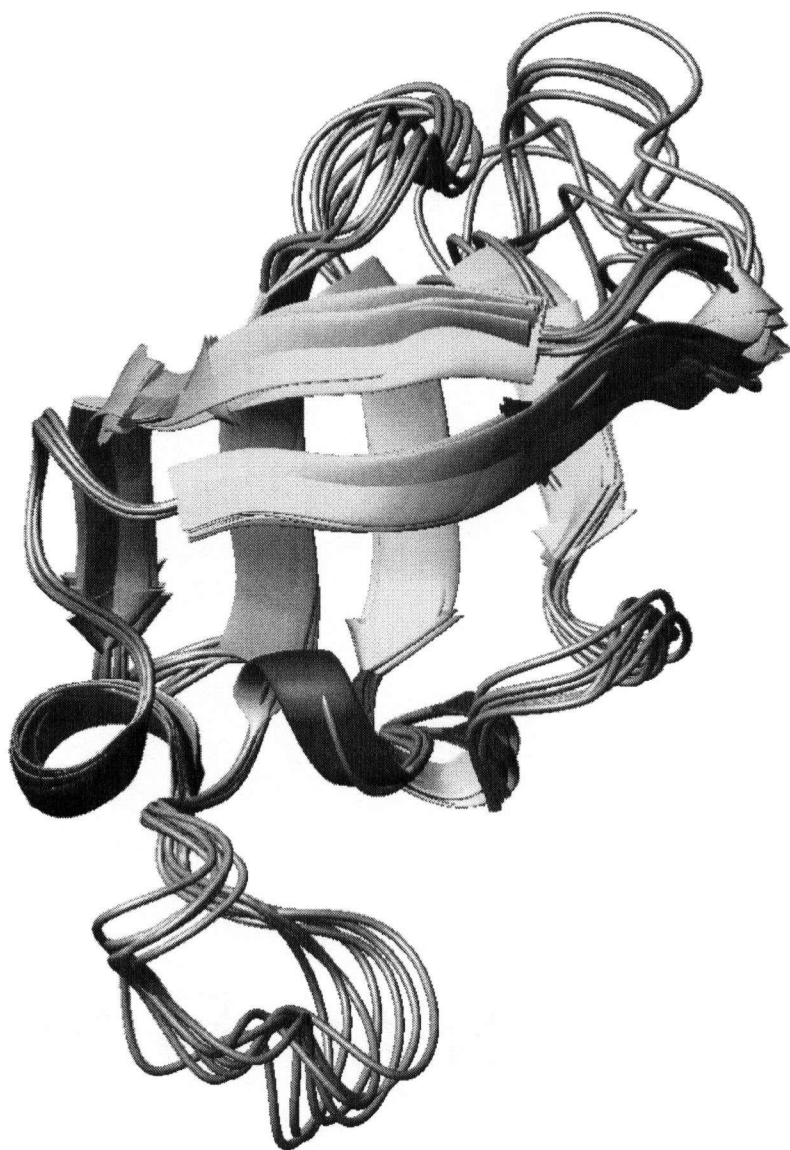
Figure 9: The peptide backbone solution structure of the S1 domain of RNase E as determined by Dr. Mario Schubert and Dr. Lawrence McIntosh by NMR. This is a superposition of 7 different best fit structures with β-sheets shown as flat bands ending in arrows pointing in the carboxy terminal direction and α helices as flat bands without arrows. Structures with the least defined structure which show the most variation between possible structures and which are therefore considered to be the most dynamic are indicated only by the grey lines .

the determination of the x-ray crystal structure of this domain (Figure 10). The native and Pb-derivative diffracted to 1.8 Å and 2.0 Å resolution, respectively. The Rwork / Rfree for the determined structure is 0.189. This structure provides a structure with greater resolution and provides some additional evidence that the S1 domain of RNase E may dimerize specifically.

3.1.5 Dimerization

Interestingly the asymmetric unit of the crystals of the RNase E S1 domain included two monomers (Dr. Schubert, personal communication). Moreover, NOE's (Nuclear Overhauser Effect) from the NMR structure were consistent with intermolecular interactions between monomers. These interactions lie on a surface of the domain separate from the putative RNA interaction sites located on β-1 and β-4. NOE's and concentration-dependent chemical shifts implicated residues Y42, I46, E76, E99, V100, and Q103 (Dr. Mario Schubert, personal communication). These observations suggest that the RNase E S1 domain may dimerize specifically. In support of this notion, the NMR tumbling time is concentration dependent, 7.4 ns at 0.6 mM and 8.3 ns at 1.2 mM, and is somewhat slow for a 10kDa monomer [95]. In contrast, static light scattering suggested that purified RNase E S1 domain is monomeric (data not shown).

To investigate the possibility that the S1 domain of RNase E multimerizes in solution, crosslinking experiments were performed with glutaraldehyde (see Materials and Methods, section 2.7.8). The gels in Figure 11 shows that prior treatment of either the wild type or *rne-1* RNase E S1 domains produces additional bands around 26kDa in lanes 8 and 9 denoted by the arrow in the margin. Visual inspection suggests that as much as 10 - 15% of the protein was converted to the putative dimer under the
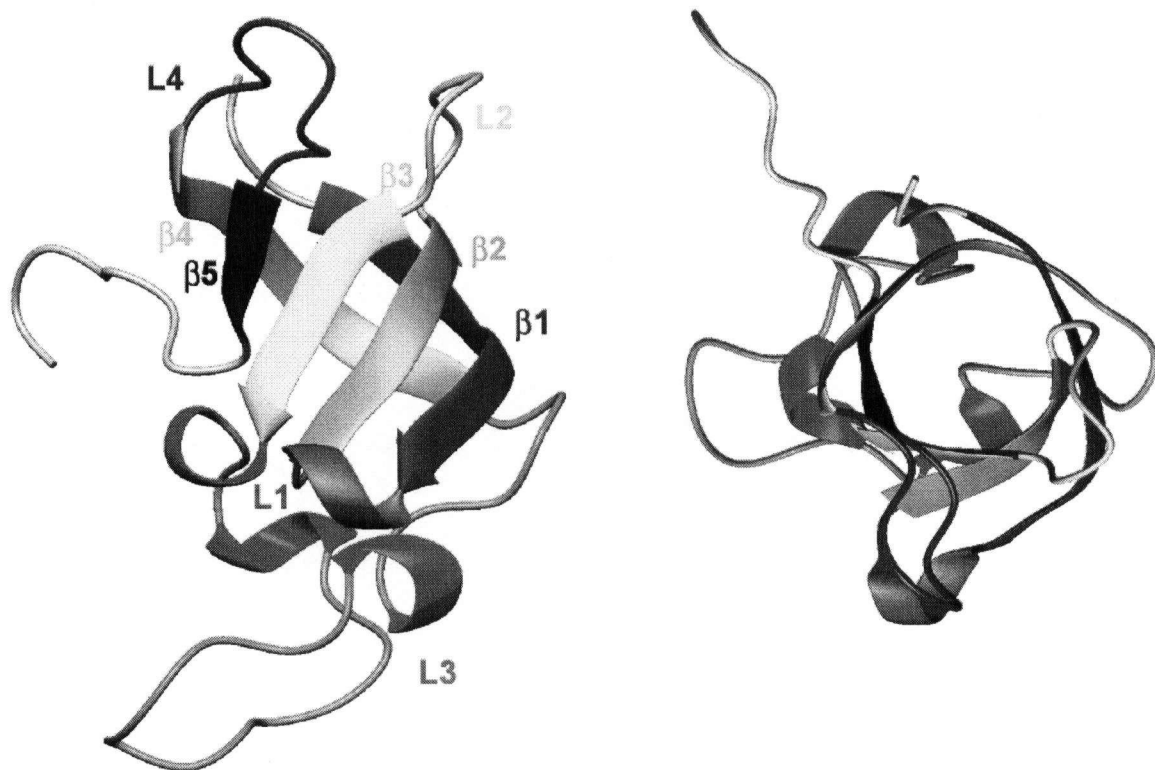
Figure 10: The crystal structure of the S1 domain of RNase E. A: The structure with labelled β-sheets and loops. The N terminus of the protein is the end nearest to β-sheet labelled β1. For the labels on the figure β is the prefix for β-sheets and L is the prefix for the loops in between the sheets. An axial view of the β-barrel as seen from the top of A. This figure and the data used to produce it are the work of Dr. Mario Schubert.
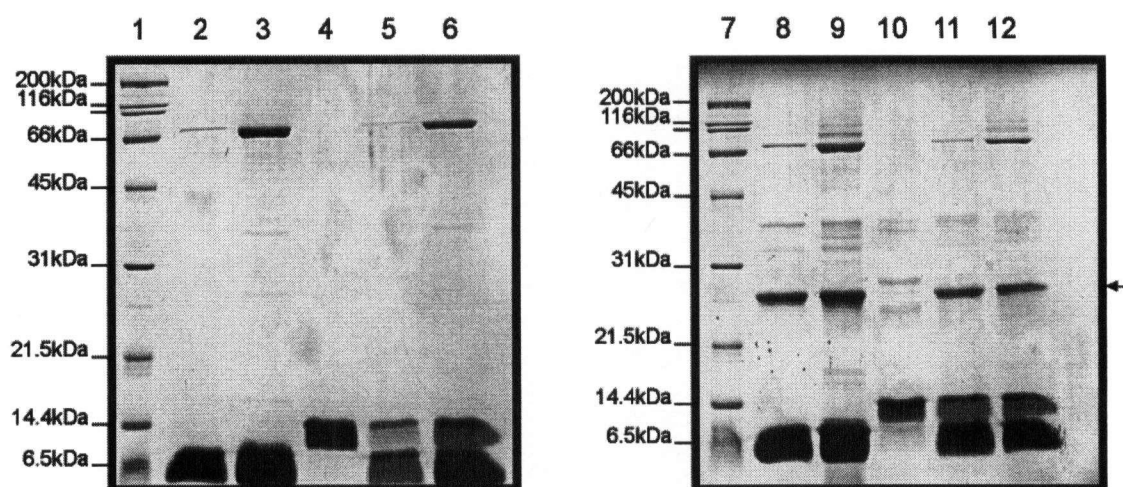
Figure 11: Crosslinking various S1 domain preparations. Samples of the RNase E S1 domain and its *rne*-1 counterpart were crosslinked in 0.01% glutaraldehyde (see section 2.7.8). Samples containing 2.25 nmol were separated on a 15% SDS-PAGE gel and stained (see Materials and Methods, section 2.7.6). Lanes 1 and 7 contain standard molecular weight markers; lanes 2 - 6 contain the various preparations without glutaraldehyde; lanes 8 - 12 are the same preparations crosslinked with glutaraldehyde. Lanes 2 and 8 contain the wild type RNase E S1 domain; lanes 3 and 9 contain the *rne*-1 S1 domain; lanes 4 and 10 contain the S1 domain of PNPase; lanes 5 and 11 contain a 1:1 mixture of wild type RNase E S1 domain and the S1 domain of PNPase; and lanes 6 and 12 contain a 1:1 mixture of *rne*-1 S1 domain and the S1 domain of PNPase. The arrow (←) in the right margin denotes the position of the putative S1 dimer.

conditions tested. Comparable treatment of the PNPase S1 domain results in a much weaker band, showing that cross-linking efficiency depends on the particular S1 domain examined. preparation around 28kDa in lane 10. Lanes 11 and 12 of figure 11 show similar bands as those in lanes 8 and 9 suggesting that heterologous crosslinking is inefficient in mixtures of S1 domains from RNase E and PNPase. Thereby demonstrating the specificity of cross -linking of the S1 domain of RNase E.

3.1.6 RNA binding studies

3.1.6.1 Filter binding studies

To determine the binding properties of the RNase E S1 domain, a two membrane filter binding assay protocol was used to permit quick analysis of many samples using a 96 well dot blot apparatus (see Materials and Methods, section 2.9). This method facilitated the examination of various factors that are involved in binding of this domain to RNase E substrates as well as the specificity of this interaction both with regards to substrate and to particular residues on the domain.

In these experiments the K_d is defined as the concentration of one component at which 50% of the other component of the interaction is bound. For these experiments the RNA concentration is limiting (4 nM) and the protein concentration is varied above and below the K_d (see Materials and Methods, section 2.9).

The value of the K_d is a reflection of the strength of the interaction between the two components, the higher this value the weaker and more transient the interaction. Thus differences in the dissociation constant provide a way of quantifying the various contributions of different factors involved in the binding interaction. Factors whose role

in binding were investigated include the 5' phosphorylation state of the RNA, the sequence of the RNA molecule, pH, salt concentration and magnesium concentration.

3.1.6.2 pH effects on RNA binding

Based on its sequence, the pI of the RNase E S1 domain is calculated to be 8.2. This relatively high pI indicates that the positive charge at physiological pH of this domain could offer strong contributions to binding the phosphate backbone of RNA. In order to examine the contribution of ionizable side chains to the interaction, the filter binding assay was performed in FAB buffer at varying pH (see Figure 12). The plot of Figure 9 shows a distinct dependence of binding on solvent pH. These data indicate that charge interactions are essential for binding because as the pH approaches the pI of the domain where the net charge is neutralized, the interaction is eliminated.

3.1.6.3 Ionic effects on RNA binding

As an alternative method to probe the importance of change interactions between the S1 domain and an RNA ligand, the filter assay was performed in the presence of varying KCl concentrations. Potassium and chloride ions in the binding buffer are able to neutralize charges on the protein and on the RNA phosphate backbone, thereby competing for ligand binding. Additionally, by increasing the ionic strength of the buffer, these ions favour hydrophobic interactions. Thus this assay enables a rough method of determining which forces dominate the interaction of the two molecules. Results of such an experiment are graphed in Figure 13. These data indicate that increasing the ionic strength of the solvent with KCl decreases the affinity of the RNase E S1 domain for the substrate RNA. Thus, data from filter binding
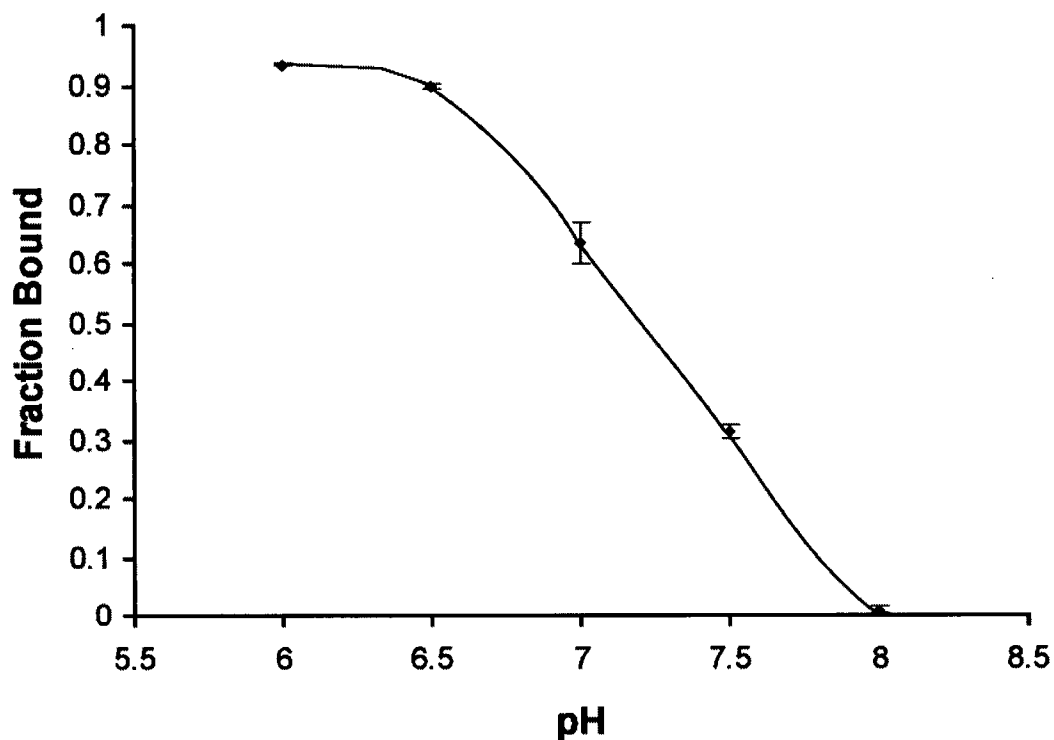
Figure 12: Effect of pH on RNA binding by the RNase E S1 domain. Filter binding assays were performed and the fraction bound was calculated as described in Materials and Methods (section 2.9). These assays were done in sodium phosphate buffer at various pH with 6 µM RNase E S1 domain. The RNA substrate is 4 nM triphosphorylated SL9A (Materials and Methods, section 2.8.2). Each point represents an average of two experiments.
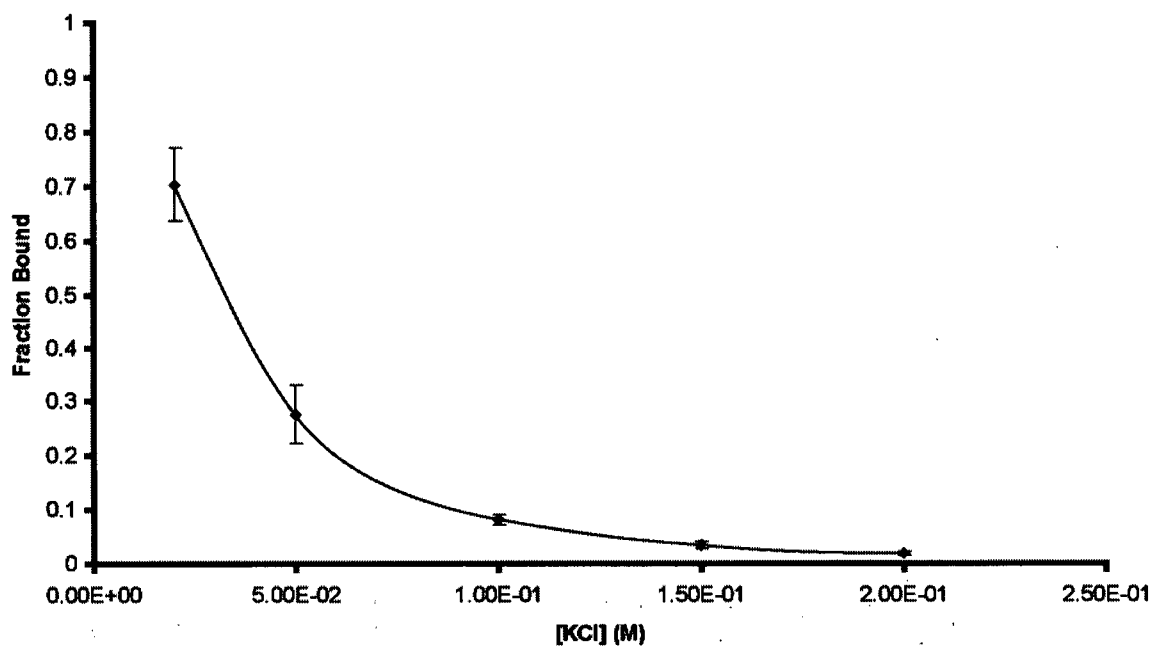
Figure 13: Effects of varying KCl concentration on the binding of SL9A by the RNase E S1 domain. Filter binding assays were performed as described in Materials and Methods, section 2.9. The protein concentration was maintained at 6 μM while the potassium chloride concentration was varied from 20 mM to 200 mM. The Fraction Bound is plotted against the KCl concentration with standard error bars and the solid line connecting each point is an approximation of a best fit line.

experiments performed with varying pH or KCl concentration confirm the importance of ionic interactions for binding of RNA to this domain.

3.1.6.4 Effects of Mg^{++} on RNA binding

The impact of divalent cation in the binding interaction was also investigated. RNase E activity requires the presence of divalent metal ions [38]; therefore, I tested whether the binding of the S1 domain to substrate might be the source of this requirement. Figure 14 shows the fraction of bound RNA is plotted versus Mg ion concentration in a standard filter binding assay. Altering the magnesium chloride concentration in the binding assay does not change the fraction bound significantly over a range of $[Mg^{++}]$ between 0 – 4mM. Since the examined interaction does not require the presence of magnesium ions, binding of RNA by the S1 domain is not the source of the requirement of magnesium ions for the catalytic activity of RNase E.

3.1.6.5 Monophosphorylation and triphosphorylation effects on RNA binding

If the S1 domain of RNase E facilitates higher enzymatic activity on monophosphorylated substrates, then the domain may have a lower K_d for such RNAs. This was tested in a filter binding assay in which the binding of SL9A RNA containing a 5' -monophosphate was compared to the same RNA molecule initiated with a 5' - triphosphate. The synthesis of these RNA molecules is described in Materials and Methods (sections 2.8.2 and 2.8.3). Monophosphorylated SL9A (■) and triphosphorylated SL9A (•) each exhibited apparent K_ds of approximately 4×10^{-6} M (Figure 15). These results indicate that the domain exhibits no preference for monophosphorylated RNA. Moreover, the S1 domain also displays very similar K_d for

47
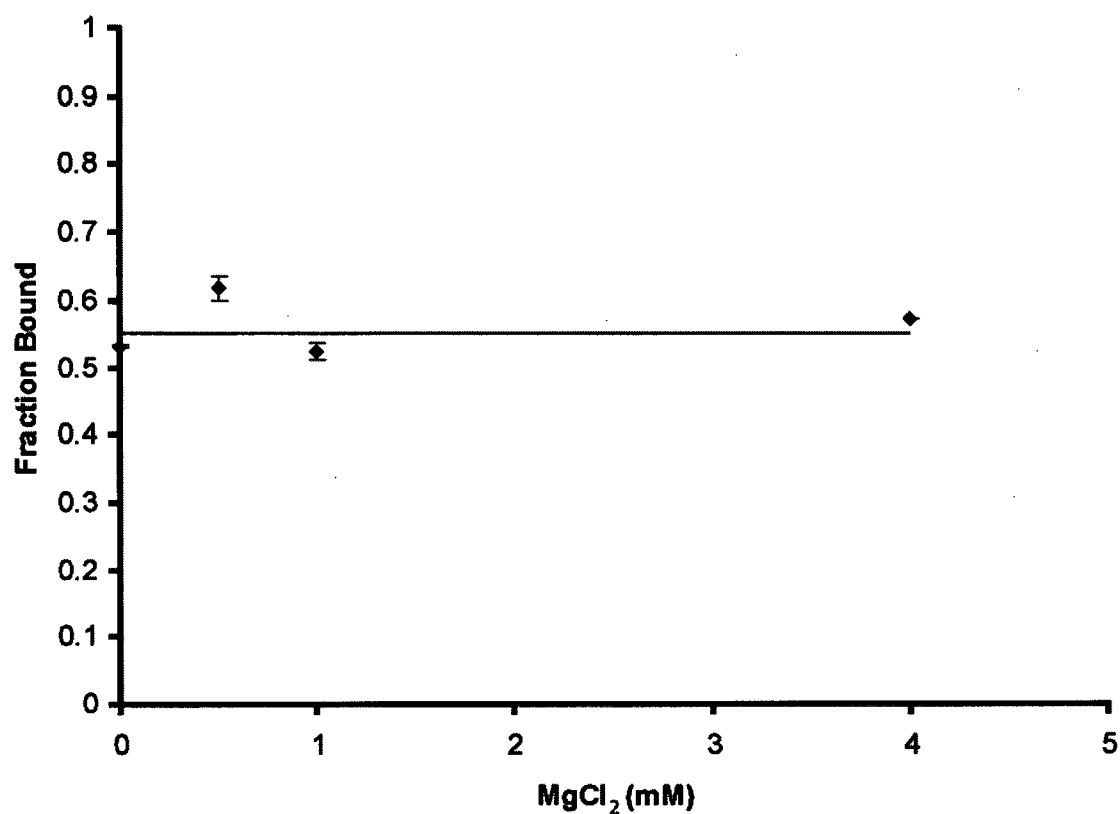
Figure 14: Effects of Mg ion concentration on RNA binding to the RNase E S1 domain. The fraction of bound RNA was determined by the filter binding assay described in Materials and Methods (section 2.9) . The concentration of RNase E S1 domain was held constant at 6 mM, the concentration of RNA at 4 nM, while the concentration of magnesium chloride was varied as indicated from 0 - 4 mM. Data points are an average of two experiments.
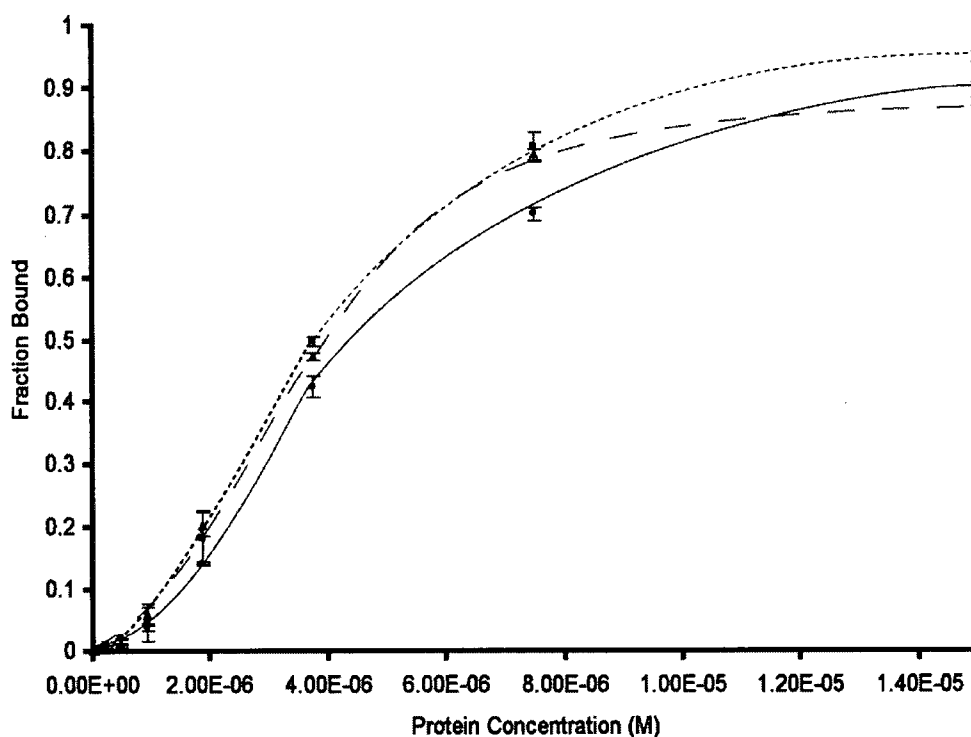
Figure 15: Binding of monophosphorylated SL9A, triphosphorylated SL9A and monophosphorylated SL9 by the RNase E S1 domain. The concentration of RNA substrates in the filter binding assay was 4 nM. The structure of the RNA is described by Spickler and Mackie (2000) [92] and its preparation is described in section 2.8.2. The concentration of the RNase E S1 domain protein is plotted against the average fraction of bound RNA from three replicate experiments. The fraction bound was calculated as described in Materials and Methods (section 2.9). A line connects each data point; a solid line for triphosphorylated SL9A; a dotted line for monophosphorylated SL9A and a dashed line for monophosphorylated SL9.

monophosphorylated SL9 (▲) RNA, indicating that the 30 adenylate residues at the 3'

end of the molecule do not impact the interaction (Figure 12).

To examine the possibility that the S1 domain of RNase E exhibits some

sequence preference, the affinity of the domain for different homopolymeric RNAs was

examined. The results plotted in Figure 16 show that both poly (U) (■) and poly (A) (♦)

exhibit apparent K_d values of approximately 2 x10^{-6} M. Moveover, the binding curves are

virtually superimposable. These results suggest that the RNase E S1 domain does not

display any specificity for one homopolymer relative to the other.

3.1.6.6 Effects of the temperature-sensitive mutation, G66S, on RNA binding.

To investigate the effect of this mutation on RNA binding, filter binding assays

were performed to compare the wild type to the *rne-1* mutant domain. The data in

Figure 17 show that the wild type S1 domain exhibits an apparent K_d for SL9A RNA of 5

x10^{-6} M, slightly higher than measured in Figure 15. The *rne*-1 mutant domain exhibits a

slightly lower apparent K_d of approximately 2 x10^{-6} M. A similar assay was performed

using end-labelled poly (C) at different temperatures to check the RNA binding capacity

of the *rne-1* mutant domain. As can be seen from Figure 18 the binding capacity of the

mutant domain for poly C RNA appears largely unaffected by temperature. The wild

type domain appears to display limited binding, especially at higher temperature (Figure

18, row 3 and row 5). However, as noted in section 3.1.1.1 the preparation of this

domain contains RNase activity. At the higher concentrations and higher temperatures

this activity may be increased resulting in degradation of the RNA and a loss of signal

on both membranes.

50
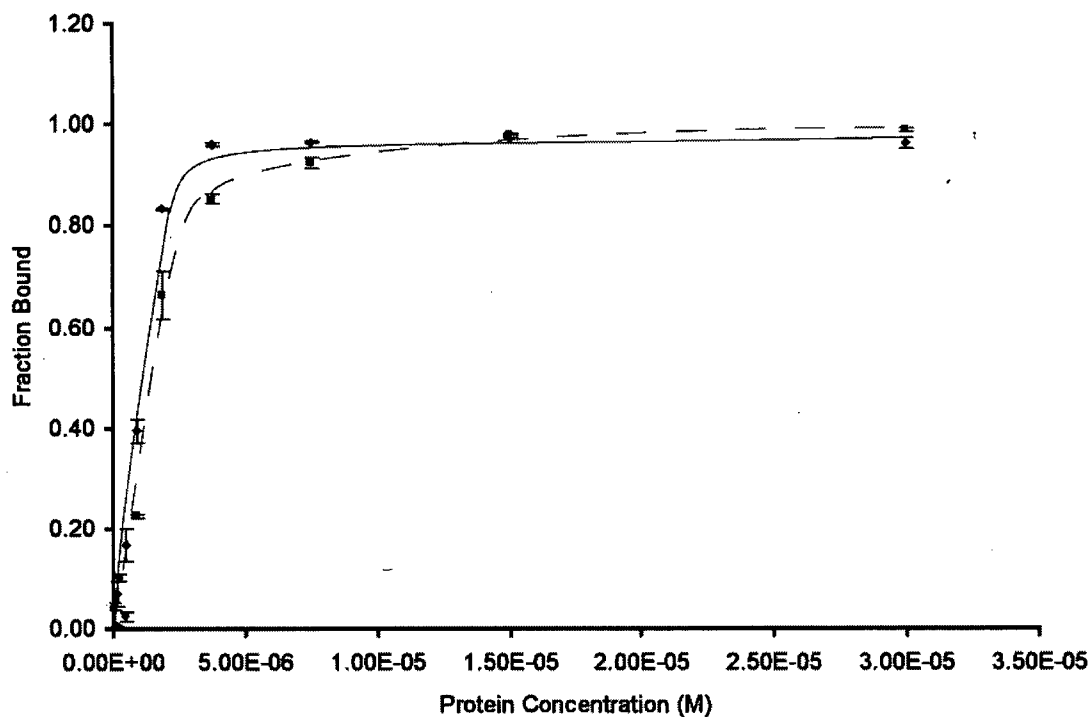
Figure 16: Binding of end-labelled homopolymeric RNA to the RNase E S1 domain. The fraction bound was determined for each protein concentration by dot blot filter binding assay as described in Materials and Methods, section 2.9. The end-labelled homopolymeric RNA, at a concentration of 4 nM, was prepared as described in Materials and Methods, section 2.8.4. The solid line (poly (A)) and dashed line (poly (U)) are approximations of a best fit line.
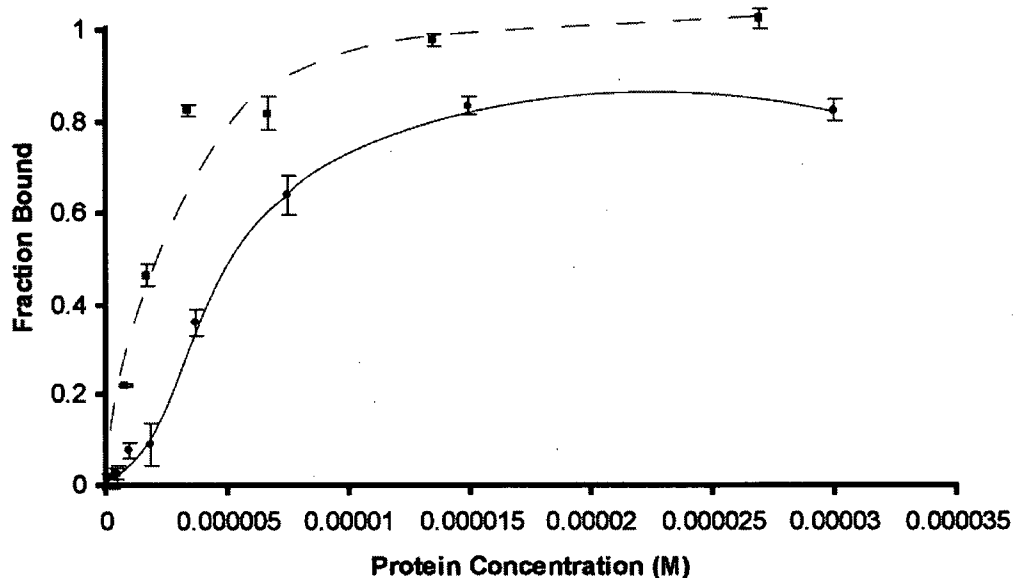
Figure 17: Binding monophosphorylated SL9A RNA to wild type (solid line) or me-1 (dashed line) S1 domains. SL9A RNA, at 4nM in binding mixture, was prepared as described in 2.8.2. Protein concentrations are plotted against the fraction of RNA bound (see Materials and Methods, section 2.9). This data is representative of three aliquots of the same dilution in three different wells of the 96-well plate for each spot. The fraction bound is an average of the signals with standard error shown as the Y-axis error bar and lines connecting data points as an approximation of best fit lines.
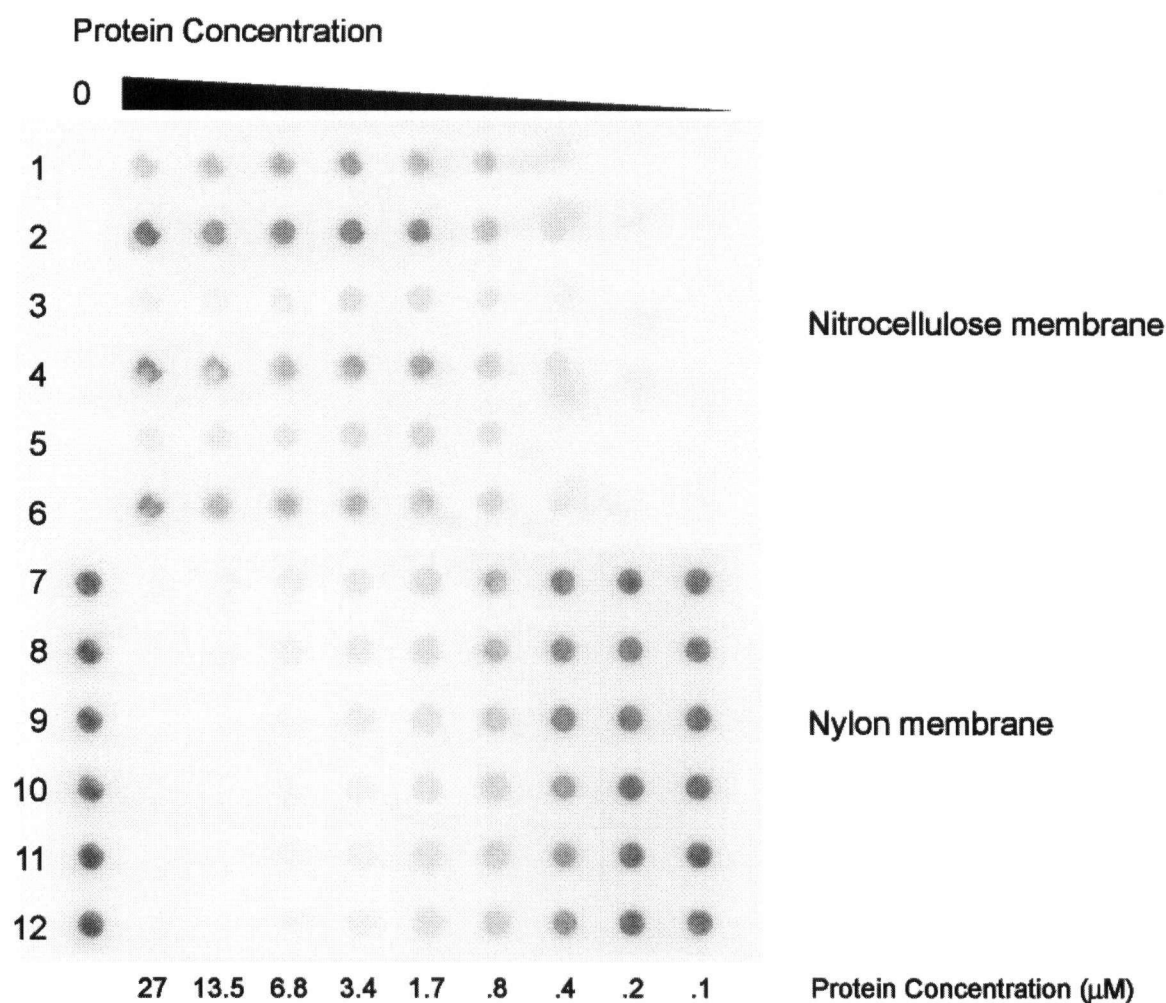
Figure 18: Binding of poly (C) to wild type or *rne*-1RNase E S1 domain. The
nitrocellulose, retaining bound RNA, and nylon membranes, retaining free RNA are
shown. Filter binding was performed as described in the Materials and Methods
(section 2.9). Odd numbered lanes contain a dilution series of the wildtype S1
domain while even numbered lanes are a dilution series of *rne*-1 S1 domains from
27μM to 0.1μM as indicated below the nylon membrane blot. The first column is a
control containing no protein. Lanes 1 and 2, 7 and 8 of the experiment were done
at room temperature; lanes 3 and 4, 9 and 10 were incubated first at 44 °C for 10
min and then transfered to ice for 10min before being applied to the well; lanes 5
and 6, 11 and 12 were incubated at 44 °C for 10min and then directly applied to the
well.

3.1.7 Competition

The hypothesis that the S1 domain of RNase E provides preference for 5' - monophosphorylated over 5' triphosphorylated substrates provided another testable property of the domain. First, the activity of RNase E should be hampered in the presence of a domain that binds to substrate molecules leaving them protected from endonuclease activity. This effect would be exacerbated if the domain binds to the same substrate recognition sites as the complete enzyme. Also, if indeed the S1 domain provides specificity by preferentially binding RNA molecules at the 5' -end, then in the presence of excess autonomous S1 domain the end-dependent activity of RNase E may be reduced. The results of such a mixing experiment are shown in Figure 19. Full length 9S RNA, labelled S, is initially endonucleolytically cleaved by RNase E at one of two sites to produce two alternative products, 8S and 7S (Figure 19, panel A). A second cleavage produces pre-5S RNA, labelled p5S. If the S1 domain mediates the 5' -end dependence of RNase E through stronger binding to monophosphorylated 9S RNA, then 8S and 7S intermediates would accumulate in the presence of competing free S1 domain. The S1 domain preparation alone displays little or no endonuclease activity. Panel C shows the effect of adding a 1, 000-fold excess of the S1 domain to the assay. The rate of formation of p5S product is not significantly different from that observed in panel A. The intensity of the p5S band in panels A and C of Figure 19 after 30 minutes are approximately equivalent. These results clearly show that even in the presence of a large excess of the S1 domain RNase E activity is unaffected.

3.1.8 DNA titration

NMR offers a powerful tool to examine the dynamics of the interaction between the S1 domain and an RNA ligand. Knowledge of the structure makes possible

54

Time (min)

| 0 | 5 | 10 | 30 | 60 | 0 | 5 | 10 | 30 | 60 | 0 | 5 | 10 | 30 | 60 |

Panel A   Panel B   Panel C

9S
8S
7S
p5S
5' end
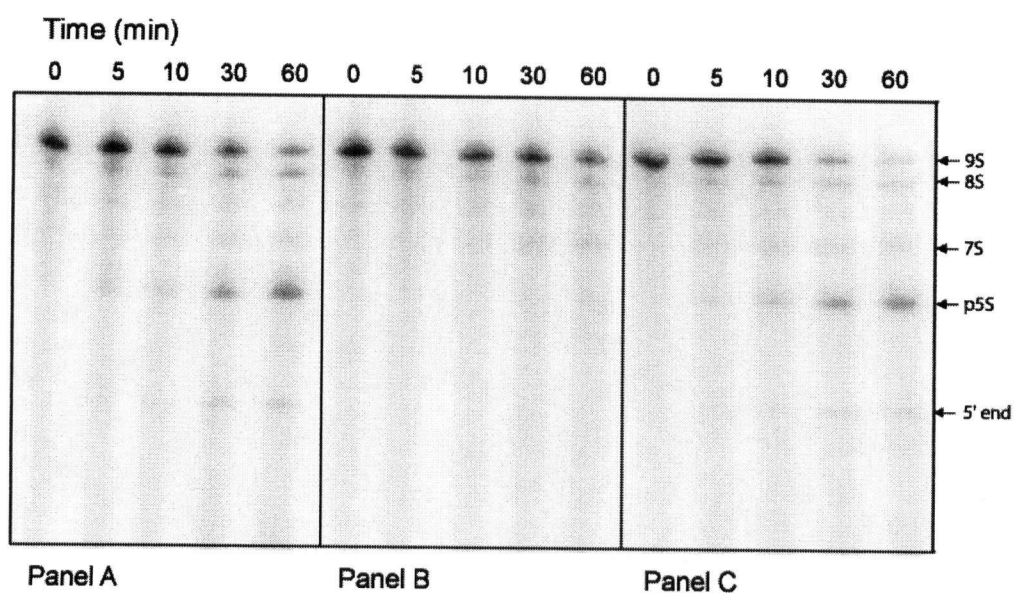
Figure 19: Time course of RNase E activity on 6.7 nM internally labelled 9S RNA transcript at 30 °C see Materials and Methods (section 2.8.6). Panel A: 2.8 nM of RNase E; Panel B; 2.8 uM S1 domain; Panel C: 2.8 nM RNase E in the presence of 2.8 uM S1 domain. (Abrevations: 9S = 9S RNA substrate, 8S = product of an initial cleavage, 7S = product of an alternative initial cleavage, p5S = pre-5S RNA product of both cleavages, 5' end = product of cleavage producing 7S)

monitoring of changes in chemical shift of specific amide backbone residues of the protein in the presence of ligand. The chemical shift of individual amide hydrogens and nitrogens reflects the environment of the residue and can be used as a sensitive indicator of changes in this environment. Therefore, an experiment was designed in which a model ligand, BR10 DNA, was titrated into a solution of the RNase E S1 domain and the chemical shifts were monitored by NMR. Residues that show a change in chemical shift during the titration are changing in position or interacting with DNA.

The ligand used for the NMR titration was a DNA mimic of a known RNA substrate (see Materials and Methods, section 2.7.2). It was observed that degradation of RNA occurred under the conditions of the NMR experiment due to small amounts of contaminating exonuclease activity that could not be removed from the protein preparation. Several additional chromatographic steps were added to the procedure in Materials and Methods (section 2.6.2) in an attempt to eliminate this activity. This is examined in more detail in section 3.1.11.

Data obtained from the NMR titration were analyzed by Dr. Mario Shubert and revealed several chemical shifts consistent with a binding interaction. These chemical shifts implicate certain residues that are potentially directly or indirectly involved in the binding of BR10 DNA. These residues and an indication of their relative change are illustrated in Figure 20 (prepared by Dr. Mario Schubert). A total of 15 residues show altered chemicals shifts on a two dimensional ^{1}H ^{15}N NMR spectrum. The amino acids are numbered as they would be in the full length RNase E protein. Several positively charged amino acid side chains are associated with these changes: R64, K71, K106, R109, and K112. Aromatic residues that appear to be solvent exposed in the NMR structure and show a chemical shift perturbation in the titration include F57, Y60 and

chemical shift perturbation
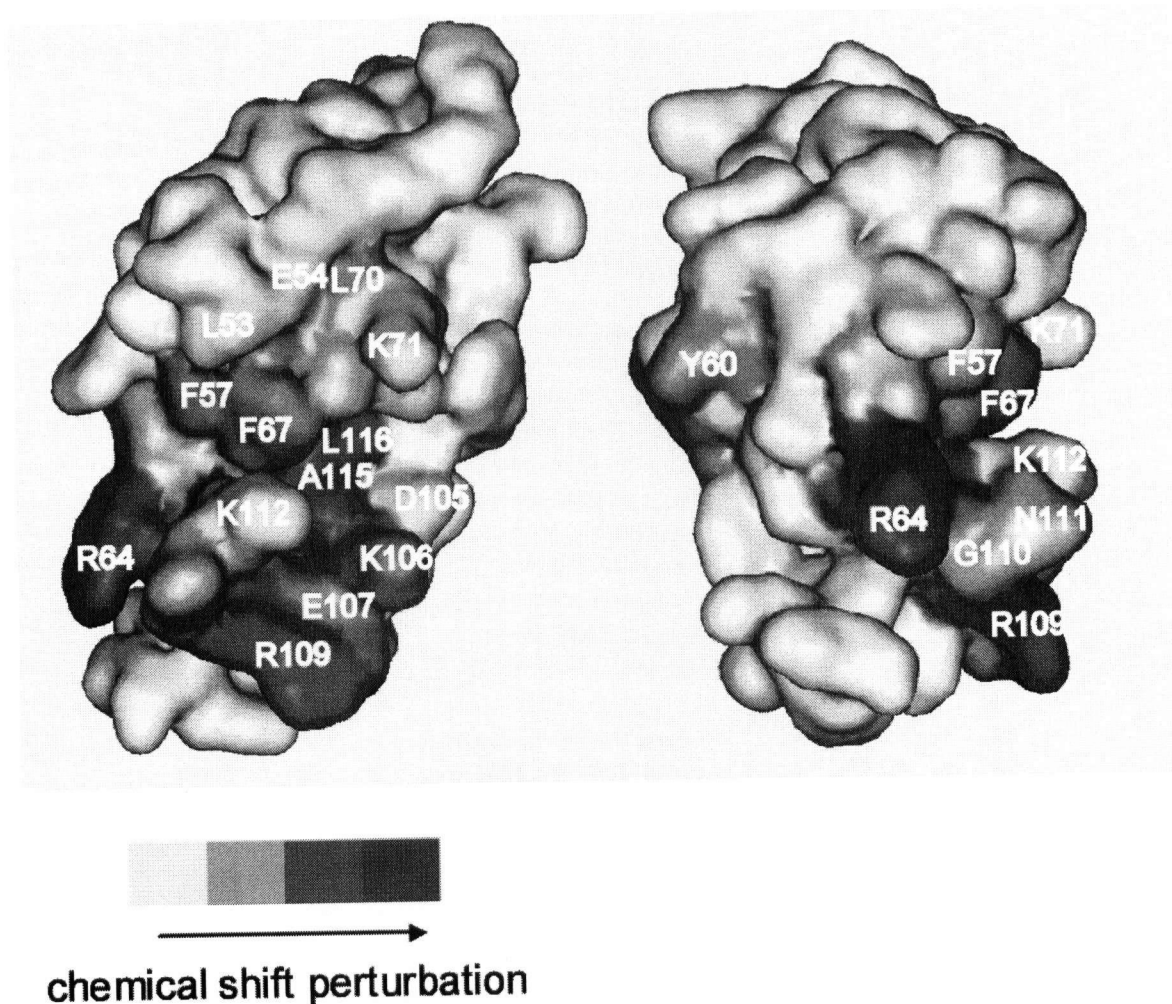
Figure 20: NMR-derived space filling model of the S1 domain of RNase E highlighting residues which show chemical shift changes upon binding to DNA. The relative change in chemical shift is indicated on the model by the shading. Those residues showing significant chemical shift perturbations upon the addition of DNA to the domain are labelled. The opposite side is shown as a 90 clockwise rotation about a vertical axis. This figure was provided by Dr. Mario Schubert.

F67. All of the chemical shift changes are localized to a single face of the domain indicating that only one side of the protein is involved in interaction with DNA, and presumably with RNA also.

3.1.9 Design of RNase E S1 domain mutants

3.1.9.1 S1 domain alignment

An alignment of the S1 domains of three enzymes of mRNA degradation in *E.coli* shows many regions of conservation (Figure 21). It is evident from the alignment that there is more conservation between the two endonucleases, RNase E and RNase G, than between RNase E or RNase G and PNPase. This may reflect the fact that RNase E and RNase G are both 5'-end-dependent endonucleases so that residues that may be important for RNase E function therefore would be more likely to be conserved in RNase G than PNPase.

3.1.9.2 Analysis of structure in terms of potential interaction residues.

A visual inspection of the structure presented in Figure 20, reveals the position of solvent exposed residues that are sterically more available for binding ligand. While residues that show a chemical shift such as A115 and L116 may provide hydrophobic pockets for the exclusion of water and interaction with bases on RNA, they also may show a chemical shift change simply from a conformational change in the backbone of the protein upon binding. Residues such as E54, D105 and E107, which also show significant chemical shift perturbation, may provide hydrogen bonding opportunities for nucleic acid bases. These residues may be providing the domain with specificity through particular hydrogen bonds to certain bases of the ligand. Therefore, a shift upon binding due to direct interaction with nucleic acid most likely implicates residues that

58

Figure 21: Alignment of three S1 domains from enzymes involved in mRNA degradation in *E.coli*. RNase E, RNase G and PNPase are labelled rne, rng and pnp respectively. The numbering system is based on full length RNase E. The alignment was calculated using Clustal W (http://clustalw.genome.ad.jp/) using a gap open penalty of 10 and gap extension penalty 0.05 and using the BLOSUM (for protein) scoring matrix. Amino acids that are conserved are highlighted in black while those only residues conserved between two domains are highlighted in grey.

protrude into the solvent and have side chains which participate in interactions with nucleic acid. Residues that showed conservation (Figure 21), a chemical shift change (Figure 20), and possessed structure and side chain properties suitable for binding DNA or RNA were designated as targets for site-directed mutagenesis, F57, R80 and R109 in particular. Phenylalanine residues can undergo hydrophobic interactions and stack with nucleotide bases in an oligonucleotide binding protein or domain [16]. Arginine residues can provide ionic interactions with the phosphate groups of the polyribonucleotide ligand to facilate binding of a protein or domain. Mutating these residues to alanine would eliminate these properties. The site-directed mutagenesis and analysis of the resultant polypeptides is described in section 3.1.10.

3.1.10 Mutant S1 domain properties

Mutant RNase E S1 domains were made using the same construct produced by Mike Cook as template (Materials and Methods). Mutants were designated by the original amino acid followed by the number of this amino acid in the full length RNase E protein sequence, followed by the amino acid replacing it in the one letter code. The mutant plasmids were sequenced and confirmed as F57A and R109A; however, the R35A mutant contained an additional unintentional mutation, E34D. Nonetheless, it was subjected to the same studies as other mutants. The mutant proteins exhibited no significant difference in solubility or concentration during their preparation. The wild type S1 domain of 10, 632Da contains 14 basic residues, and 13 acidic residues resulting in a predicted pI of 8.2. While the F57A mutation had little impact on the predicted pI of the domain, the R109A and R64A + E63D mutations altered the predicted pI based on sequence from 8.2 to 7.04.

The isolated mutant domains, R109A and F57A, were subjected to filter binding assays to examine the contributions of these residues to the binding interaction. As can be seen from the filter binding results with these mutant domains (Figure 22), there is no detectable difference in RNA binding under the conditions tested. The K_d's for both mutant domains are approximately 1 x10^{-6} which is very close to that for the wild type domain (Figure 16), within error of the experiment. Moreover, neither mutant domain showed a detectable difference in K_d for poly A compared to poly U.

3.1.11 RNase contamination

As noted in section 3.1.8, RNase activity was found in preparations of the S1 domain of RNase E. Panel A of Figure 23 shows that poly C RNA is almost completely converted to low molecular weight products after a 10 minute incubation with the wild type S1 domain at 30°C. This activity complicates assays of RNA binding and eliminated the possibility of using RNA in NMR experiments. Alternative purification techniques were utilized in an attempt to rid the preparation of the nuclease activity, including reverse phase high performance liquid chromatography (see Materials and Methods, section 2.6.2). A single, apparently homogeneous peak of an UV absorbance at 280 nm eluted from this column (data not shown); however, the resulting purified domain still contained a level of nuclease activity similar to the starting material. This result suggested that the S1 domain itself could have intrinsic nuclease activity. To test this hypothesis, the activity of the wild-type protein preparation, was compared to that of three mutants (Figure 23). After 10 min at 30°C the wild-type RNase E S1 domain has degraded the poly (C) RNA to small oligonucleotides and nucleotides whereas longer RNA persists longer in the reactions with rne-1, F57A and R109A mutants (Figure 23, Panels B, C, D respectively). Although not a quantitative assay, it can be seen that the
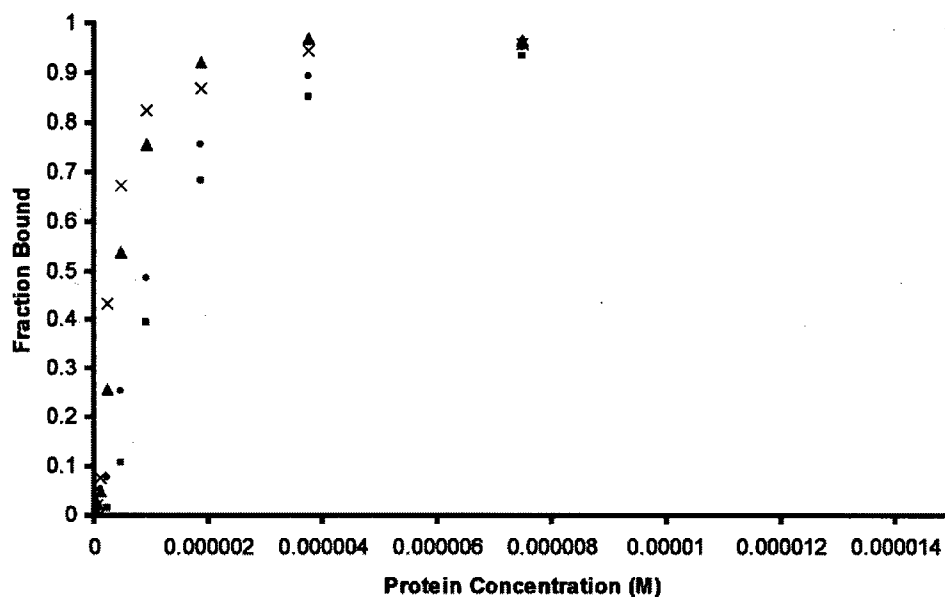
Figure 22: RNA binding by RNase E S1 domain mutants, F57A and R109A. Each protein was prepared as described in Materials and Methods (section 2.6.2) and tested for filter binding with 4 nM of end-labelled poly (A) or poly (U) as indicated. The mutant F57A was tested with poly (A) (•) and poly (U) (▪), similarly R109A was tested with poly (A) (▲) and poly U (×). The fraction bound was calculated described in Materials and Methods section 2.9. For clarity, best fit curves are omitted.
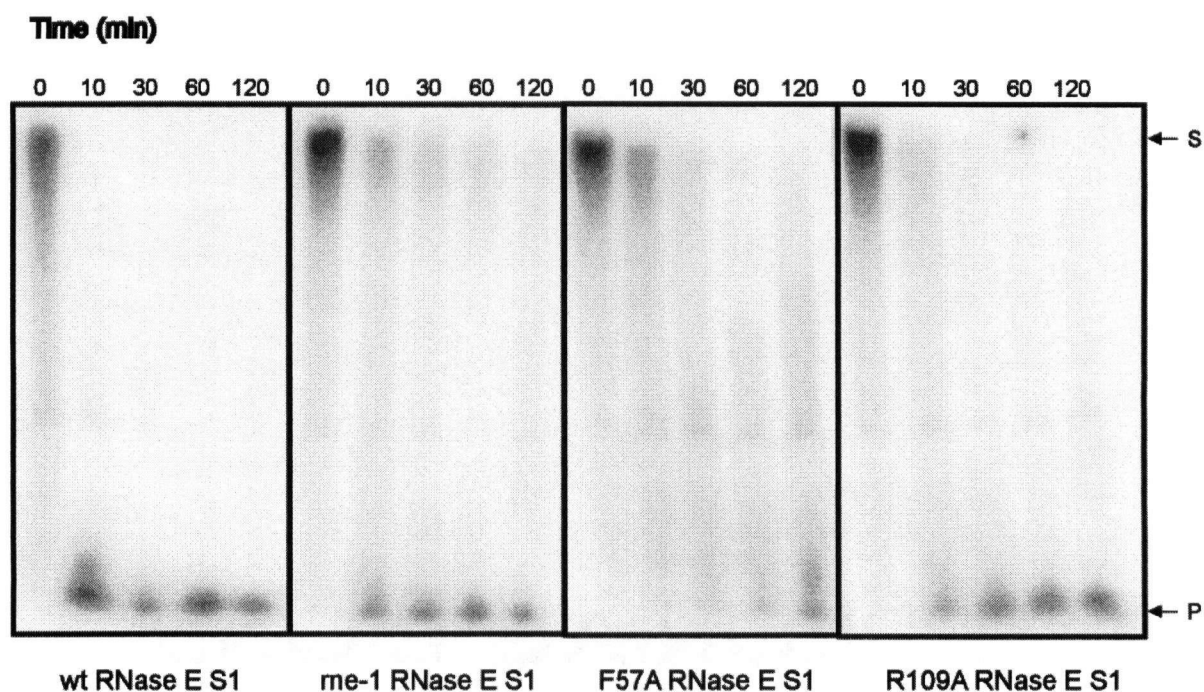
Figure 23: Nuclease activity of various RNase E S1 domain protein preparations. 5' - end labelled poly C (5 nM) was incubated with the indicated RNase E S1 domain (25 μM) for the indicated time at 30 °C. The reactions were quenched in formamide buffer and separated by electrophoresis on 8% TBE UREA polyacrylamide gels. S indicates the signal from the largest species in the gel while the P indicates the signal from the smallest fragments in the gel. (Abbreviations: S = substrate poly C RNA, P = product oligo C RNA).

rne-1 S1 domain contains the least amount of RNase activity followed closely by the F57A S1 domain mutant. It could therefore, be argued that the S1 domain exhibits nuclease activity in the absence of the full length enzyme and mutations in the domain interrupt this activity.

To investigate this further a western blot of two S1 domain preparations was used to identify potential contaminants. Both preparations contain some RNase G, shown by the arrow, but no detectable RNase E (Figure 24, top and bottom panels). As can be seen from Figure 24, middle panel, the wild-type S1 domain contains higher amounts of contaminating full length PNPase than does the *rne-1* construct. The slightly faster migrating bands are likely products of proteolysis of PNPase corresponding to the elimination of the KH and S1 domains. These domains have been shown to be sensitive to proteolysis previously and are detected by the PNPase polyclonal antibody [84] (Janet Hankins, personal communication). This would be consistent with the observed lower nuclease activity of the *rne-1* construct, if full length PNPase is the source of the RNase activity. The presence of 20mM phosphate buffer at pH 6.5 in all the preparations provides the necessary reaction conditions for phosphorylysis catalyzed by PNPase. Therefore, it is likely that at least some of the nuclease activity of the preparation is due to the contamination by this enzyme. It has not been shown conclusively, however, that the S1 domain of RNase E lacks intrinsic exonuclease activity independent of PNPase contamination or that another contaminating RNase enzyme is responsible for this activity.

3.2 PNPase S1 domain

To investigate the role of the S1 domain of PNPase in mRNA degradation in *E.coli*, a PNPase construct was made with a deletion in this domain. At the outset, it

64
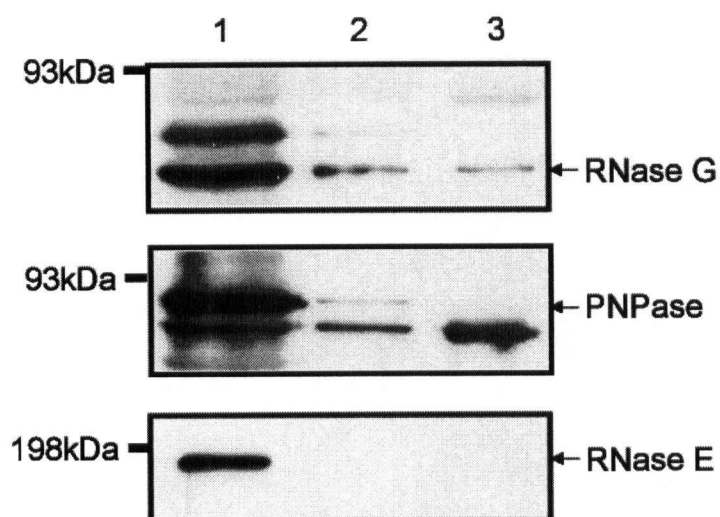
Figure 24: Western blots of RNase E S1 domains. Lane 1 contains a whole cell extract (courtesy of Dr. George Mackie); lane 2 contains the wild type RNase E S1 domain; lane 3 contains the *rne-1* RNase E S1 domain. Each blot was probed with the indicated polyclonal antibodies and visualized using a secondary antibody conjugated to horse radish peroxidase (see Materials and Methods section 2.7.7). Molecular weight markers migrated as indicated to the left of each blot.

was essential to determine whether an N terminally His-tagged PNPase would serve as a good model. This type of construct has been used before but has lacked activity in our hands [96]. It was found that the His-tagged PNPase, while active, had different properties under the conditions tested (section 3.2.1). An untagged PNPase lacking the S1 domain and a construct lacking the KH domain were assayed for activity to test the hypothesis that these putative RNA binding domains contribute to the processivity of PNPase (section 3.2.2). Additionally the PNPase lacking the S1 domain was tested for its ability to rescue the cold-sensitive phenotype of a PNPase null mutant (section 3.2.3).

3.2.1 Activity of His-tagged and untagged PNPase.

Untagged PNPase was expressed and purified from BL21 harbouring the plasmid pGC400, while the construct PEPα18 in BL21 was used for expression and purification of His-tagged PNPase (see Materials and Methods, section 2.6.1). While both preparations of PNPase showed phosphorylytic activity dependent on the presence of phosphate, there were detectable differences in the sizes of products produced from reactions with internally labelled $rpsT$ (268 – 447) poly A_{30} mRNA (Figure 25 compare lanes 6 - 10 with 16 - 20). The data show that the native enzyme is more active than its tagged counterpart. The digestion catalyzed by wild type (lanes 6 - 10) is complete within 5 minutes whereas His-tagged PNPase requires 30 – 60 min to digest all the substrate (Figure 25, lanes 16 - 20). Moreover, while wild type PNPase produces the product labelled P, the His-tagged protein produces an extended RNA product band labelled P' in addition to small amounts of P. The source of this difference is unknown as is the identity of the extended product. Accordingly, it was concluded that wild type PNPase is a more useful in $vitro$ model than the tagged enzyme.

66
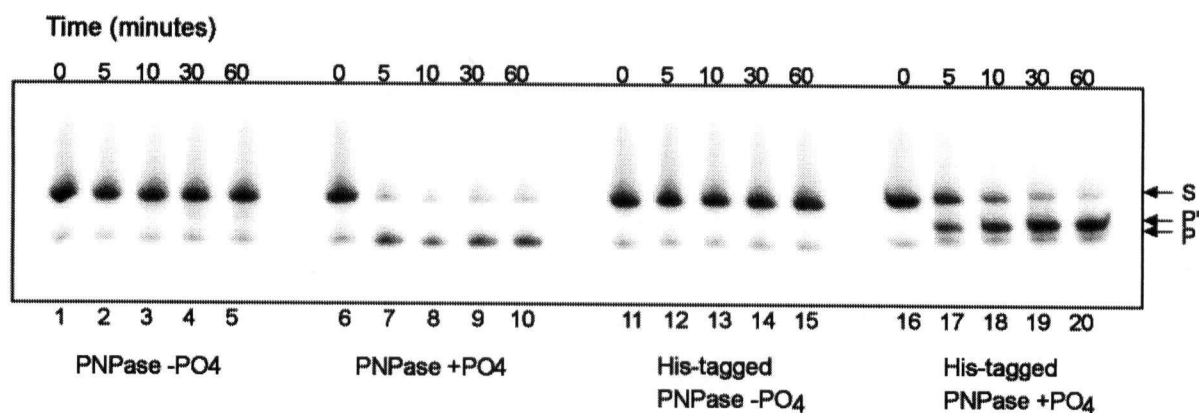
Figure 25: Rate of phosphorolysis of wild type and his-tagged PNPase. Reaction mixtures contained 0.8 pmol of internally labelled rpsT poly A mRNA, 0.8 pmol of PNPase and were incubated with and without 10 mM phosphate buffer pH 7.5 as described in Materials and Methods (section 2.8.5). A representative experiment is shown where either native or hexahistidine tagged PNPase was the source of activity. (Abreviations: S = rpsT/poly A substrate, P = phosphorylysis product, P' = elongated product (see text)).

3.2.2 Processivity

To investigate the role of the S1 domain in the processivity of PNPase, two different deletion constructs were made (Figure 26). The PNPase ΔKH mutant eliminates the entire KH domain, while the PNPase ΔS1 deletion eliminates the first three β-sheets of the PNPase S1 domain. These deletion mutants have been previously designed and partially characterized by Jarrige et al. 2002 [83]. To recreate these mutants, site-directed mutagenesis was employed using primers RE16-M1, RE16-M2 and RE17-M1, RE17-M2 to generate PNPase ΔS1 and PNPase ΔKH, respectively (Table 2, section 2.4). Neither construct encoded a hexahistidine-tag. The resultant proteins were overexpressed and purified using a three step chromatographic procedure as described in Materials and Methods (section 2.6.1).

The model substrate SL9A, described previously [92], was used to assay phosphorolysis activity of the PNPase ΔS1 and PNPase ΔKH enzymes compared to the wild type PNPase. As can be seen from Figure 27 there are very significant differences in the specific activity of these different deletions. The PNPase ΔS1 (Figure 27, Panel B) can be estimated from the time course to be at least 100 -fold less active than the wild type (Figure 27, Panel A). The PNPase ΔKH mutant (Figure 27, Panel C) can be estimated to be about 20 -fold less active than the wild type enzyme shown in Panel A. No intermediates could be detected between the substrate (S) and product (P) bands even when similar samples were separated at higher resolution on a sequencing gel (data not shown). The absence of detectable intermediates indicates that all three exhibit processive phosphorylytic activity.

In the cell PNPase is under conditions that favour phosphorolysis; however, *in vitro* conditions can be designed such that RNA polymerization occurs. Both the

Wild type PNPase

PH'   PH   KH   S1

0-210   312-541   551-591 622-690

PNPase ΔKH

PH'   PH   S1

563-619

PNPase ΔS1

PH'   PH   KH   S1

625-658
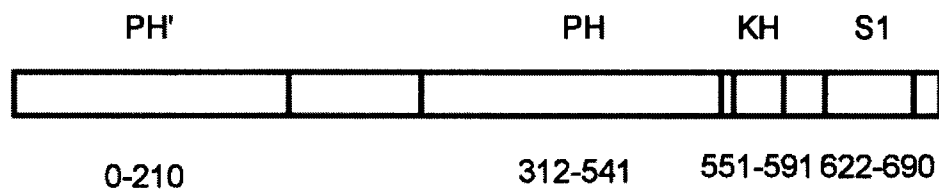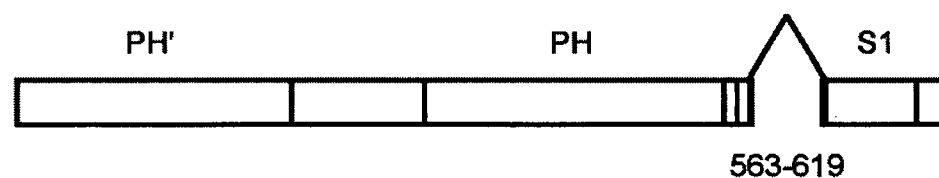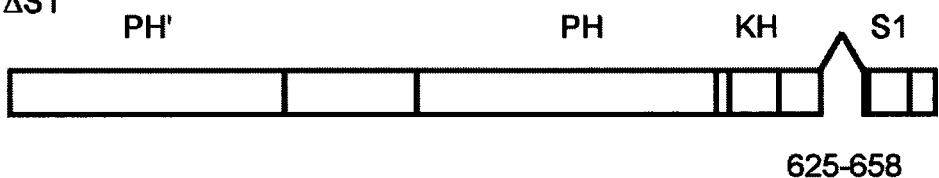
Figure 26: Schematic of PNPase wildtype and deletion mutants. Both deletions were created using site-directed mutatgenesis and confirmed by DNA sequence data (see Materials and Methods, section 2.4). The numbers in the constructs labelled PNPase ΔKH and PNPase ΔS1 indicate those residues that have been eliminated. All constructs were made in the vector pET11.
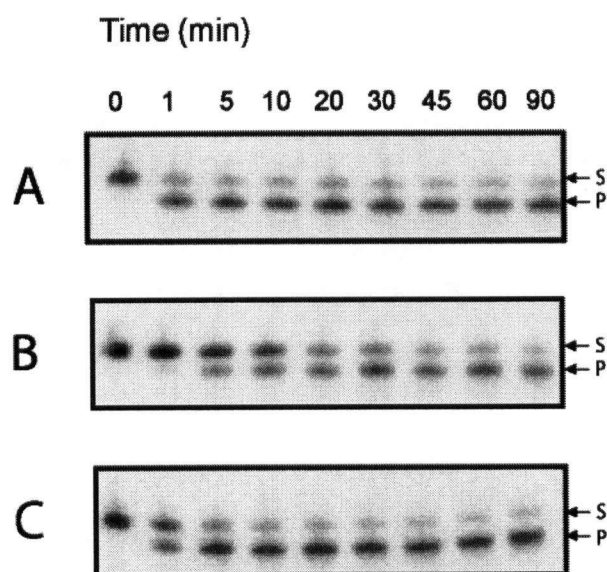
Figure 27: Rate of phosphorolysis of internally labelled SL9A RNA. Reaction mixtures contained 0.8 pmol RNA, 10mM phosphate buffer pH 7.5 and were incubated at 30 °C as described in Materials and Methods (section 2.8.5). A representative experiment is shown using 0.65 μM wild-type PNPase (Panel A), 22 μM PNPase-S1 (Panel B) and 4.5 μM PNPase-KH (Panel C). (Abreviations: S = SL9A substrate, P = phosphorylysis product).

phosphorylysis and polymerization activities were tested for processivity using the mutant PNPase ΔS1. These results are shown in Figure 28. Panel A shows no detectable intermediates. Unfortunately under these conditions the reaction occurs too quickly to conclude that no intermediates would be detected. It is clear, nonetheless, that the S1 domain of PNPase is not necessary for either activity of PNPase under the conditions tested.

3.2.3 Cold-sensitive phenotype of *pnp* mutants.

As the S1 domain closely resembles a cold shock domain and a PNPase deletion strain of *E.coli* shows a cold-sensitive phenotype, the PNPase ΔS1 plasmid was tested for its ability to rescue this phenotype. Figure 29a - c shows that a PNPase deletion strain (pnp::Tn5) is viable at 37°C. When this strain contains a plasmid with an antisense insert it does not show growth when cultured at 16°C (Figure 26 e). A wild type PNPase construct can rescue the cold-sensitive phenotype of this strain and the culture is viable at low temperature (Figure 29 d). The PNPase ΔS1 construct cannot rescue growth of the mutant and exhibits the same phenotype as the negative control (Figure 26 f).

3.2.4 Filter binding assay

The S1 domain of PNPase (corresponding to residues 617 - 700) was overexpressed and purified as described in section 2.6.2. Results from the purification procedure were followed by separating samples from intermediate steps in the procedure on an SDS-PAGE gel (see Materials and Methods, section 2.7.6); (Figure 30). The purified protein is shown in Figure 30 B Lane 2 and appears free of detectable contaminants. The smear in this lane is thought to be from overloading the gel.
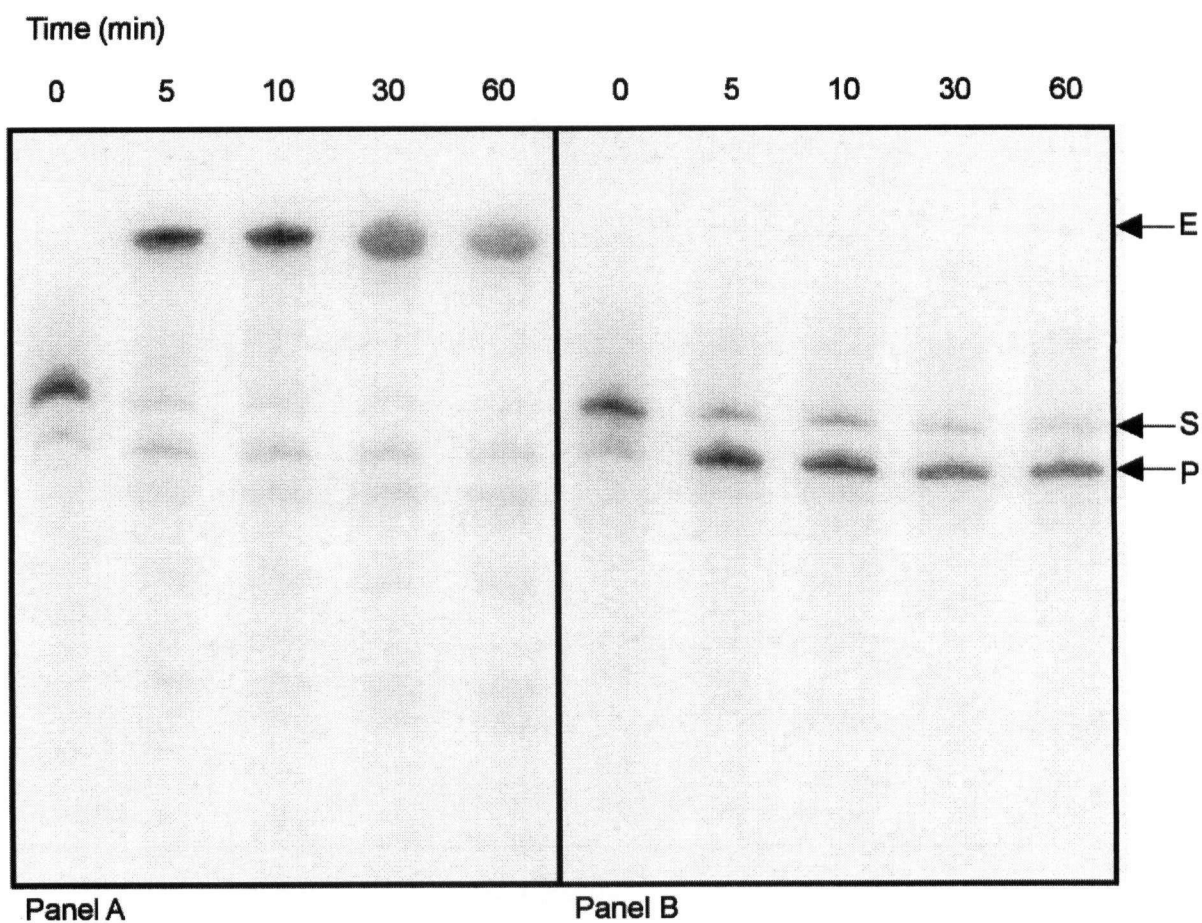
Figure 28: Rate of phosphorylysis and homopolymer tailing by PNPase ΔS1. Reaction mixtures contained 0.8 pmol of internally labelled rpsT poly A mRNA and 2.3 μM PNPase-S1 incubated in the presence of 3 mM ADP (Panel A) or 12 mM sodium phosphate buffer pH 7.0 (Panel B). (Abbreviations used: S = substrate, E = extended RNA, P = phosphorylsis product.)

a: PNPase   b: PNPase ΔS1   d: PNPase   e: PNPase ΔS1
                   antisense   antisense

c: PNPase ΔS1   f: PNPase ΔS1

LB agar at 37 degrees   **LB agar at 16 degrees**
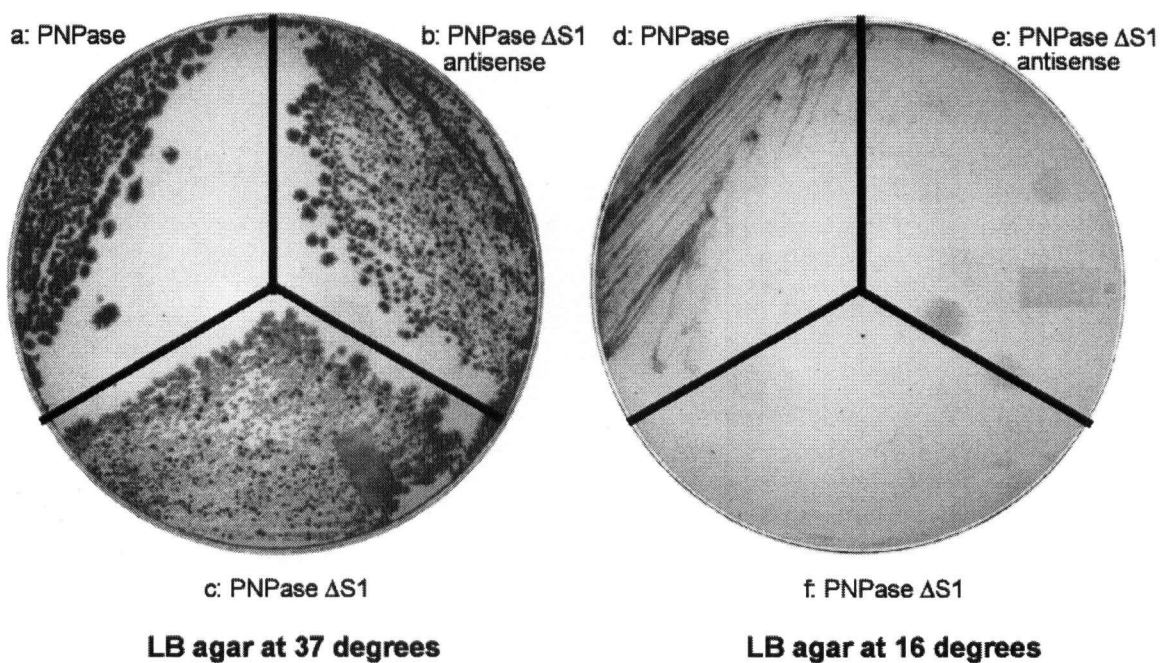
Figure 29: Rescue of the cold-sensitive phenotype of PNPase null mutants by wild-type or PNPase-S1 constructs. *E. coli* pnp::Tn5 transformed with plasmids pGC400, containing full length PNPase (a, d), pRE75 (PNPase ΔS1) (c, f) or pRE74 (PNPase ΔS1 ligated in the vector in the opposite orientation) (b, e) were plated on LB agar containing 100ug/mL ampicillin. Plates were incubated at 37 and 16 degrees.
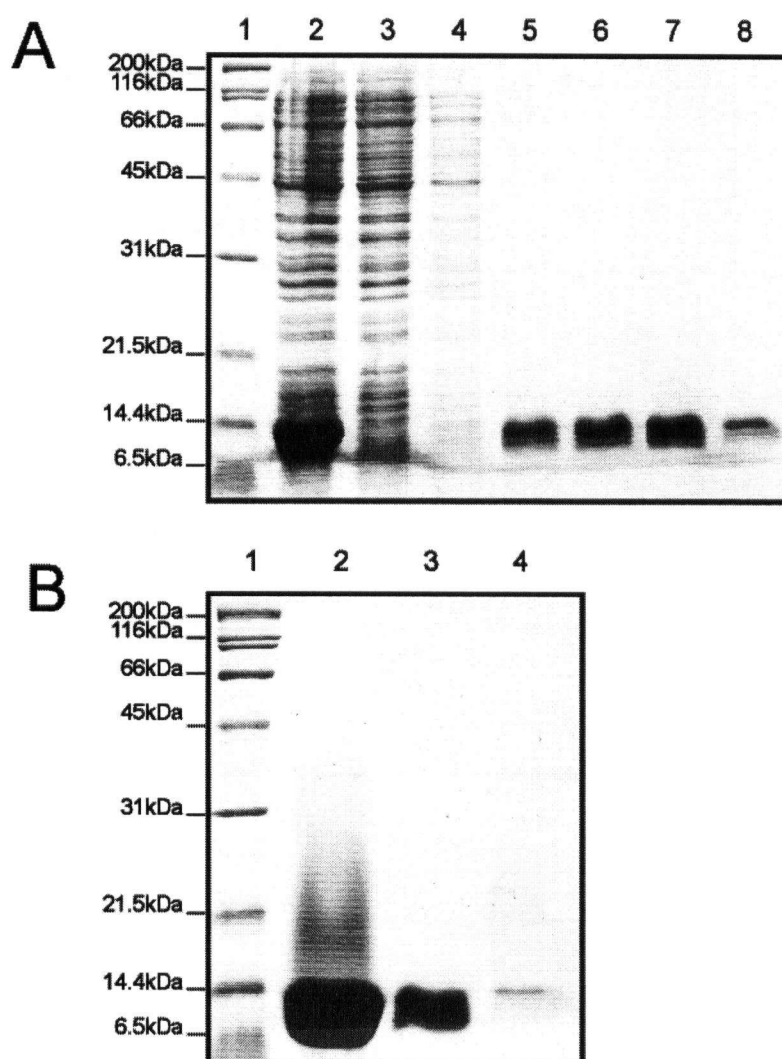
Figure 30: Purification of the S1 domain of PNPase. The S1 domain of PNPase was purified as described in Materials and Methods (section 2.6.2). Various fractions were separated on a 15% SDS-PAGE gel (see Materials and Methods section 2.7.6). A: Lane 1, Molecular size markers (sizes of each marker are indicated to the left); Lane 2, the S30 fraction; Lane 3, Talon column flow through of the S30; Lane 4, 5 mM imidazole wash; Lane 5, second 5 mM imidazole wash; Lane 6, 15mM imidazole wash; Lane 7, 50 mM imidazole wash; Lane 8, 500 mM imidazole wash. The fraction corresponding to Lane 7 was concentrated and dialysed overnight in the presence of thrombin as described in Materials and Methods (section 2.6.2). B: Fractions after thrombin treatment Lane 1, Molecular size markers; Lane 2, concentrated flow-through; Lane 3, flow-through Lane 4; 500 mM imidazole wash.

74

The ability of the purified PNPase S1 domain to bind RNA was also examined using a filter binding assay. Both SL9A and SL9 RNAs were tested in either monophosphorylated or triphosphorylated form (Materials and Methods, section 2.9). The K_d of the PNPase S1 domain was estimated to be over 200 μM (data not shown). Thus, this domain exhibited a much higher K_d than the S1 domain of RNase E.

4 Discussion

This thesis has addressed many questions about the function of S1 domains in two key enzymes of mRNA degradation in *E.coli*. The importance of this domain is evident from its presence in multiple enzymes involved in this fundamental process (see Figure 2).

Two basic hypotheses were tested in this thesis. It was thought that these domains served different functions in RNase E and PNPase through their ability to bind RNA. In RNase E the S1 domain was hypothesized to bind to substrate mRNA molecules and provide the phosphate binding pocket that enhances RNase E activity against monophosphorylated RNA substrates. In PNPase the S1 domain was hypothesized to bind to substrate mRNA molecules separately from the active site of the enzyme and therefore impart processivity to its exonuclease activity. In short this work has shown that both of these hypotheses will need revision.

A simple scheme for the purification of hexahistidine-tagged S1 domain of RNase E or PNPase has been established and has proven to be effective in purifying each protein in sufficient quantities to permit strcutural investingations.

4.1 Function of RNase E S1 domain

4.1.1 RNA binding

Although studied in isolation from the intact enzyme, the S1 domain is implicated in playing a role in binding substrate RNA to full length RNase E. The results from the NMR titration of the domain with nucleic acid, although represented graphically in Figure 17, clearly showed that the change in chemical shifts followed a sigmoidal titration

curve. This result indicates that this is a genuine binding interaction as it is saturable. In addition, the localization of these altered chemical shifts to one area of the structure confirms that this interaction is specific. Filter binding results also quantify the interaction of the S1 domain of RNase E with SL9A RNA molecules (Figures 12 and 13). These experiments estimate a K_ds of between 1 and 2 μM. This apparent K_d is consistent with those of cold shock domain proteins from the Csp A family. Csp B, Csp C and Csp E have K_d for binding substrate RNA in the low micromolar range (12.6 μM, 3.9 μM, and 0.9 μM respectively), consistent for a role in an RNA chaperone function [97, 98].

4.1.2 Specificity

The issue of the specificity of the RNase E S1 domain has been addressed in this work through filter binding assays. The dependance of binding on pH or KCl concentration was analyzed in two filter binding experiments (Figures 9 and 10). These experiments indicate that charge interactions are very important in the interaction of the RNase E S1 domain with substrate RNA molecules. In fact, ionic interactions may dominate over hydrophobic interactions as increasing the ionic strength weakens binding instead of strengthening it. In terms of RNase E's substrate specificity, this may indicate that the S1 domain predominately interacts with the phosphate backbone of the RNA and may not provide a means of RNA substrate recognition, as the negative charge of the phosphate backbone is sequence-independent.

Confirmation of the lack of sequence specificity of this domain is shown in Figures 13 and 14. These results show that the wild type RNase E S1 domain does not preferentially bind 5' -end-labelled poly A, poly U or poly C. While this strongly suggests that the domain does not have any broad sequence preference for binding, it does not

eliminate the possibility that there exists a specific sequence to which this domain binds with a much lower K_d. It has been shown, for example, through the SELEX method that Csp B, Csp C and Csp E have lower K_ds for particular nucleic acid sequences [97]. However, sequence-independent binding does not contradict a role for the S1 domain in the function of RNase E as an endonuclease having a general role in mRNA decay and being able to recognize many mRNAs. An alternate site on this enzyme could impart specificity for the AU-rich consensus sequences of targets. Performing a SELEX experiment using the isolated S1 domain would reveal whether the domain possesses any sequence specificity.

This thesis tested a major hypothesis that the RNase E S1 domain exhibits specificity for binding monophosphorylated RNA, thereby imparting RNase E with the observed increased activity on monophosphorylated RNA as compared to triphosphorylated RNA. The results in Figure 12 show that the domain binds to monophosphorylated and triphosphorylated SL9A with similar affinities. This suggests that the S1 domain of RNase E is not the putative phosphate binding pocket [99].

Although the stoichiometry of the interaction of the S1 domain with RNA is unknown, its size indicates that multiple domains could bind single-stranded RNA of the length used in the filter binding assays. The domain interacts with only a few nucleotides in determined structures of ob-fold proteins complexed to nucleic acids [12]. Interestingly, the stretch of 30 A residues in SL9A does not alter the K_d of binding relative to SL9 indicating that the S1 domain does not bind preferentially to the 3' -poly A tract. The data in Figure 8 do show that the domain does bind to poly A RNA. Moreover, the domain appears to bind homopolymeric RNA with the same affinity as the SL9A and SL9 RNAs. All the tested substrates, monophosphorylated SL9A,

triphosphorylated SL9A, monophosphorylated SL9 and homopolymeric RNA, share limited common properties. These include a 5' -end and 3' -end as well as some single stranded character at their 5' and 3' ends. It is conceivable, therefore, that this domain imparts the preference of RNase E for substrates with a 5' -single stranded terminus [8] but not its specificity for 5' monophosphorylated RNA (see Figure 31). Thus, this thesis has established that the putative phosphate binding pocket is independent from the S1 domain. It, however, is possible that in the context of a tetramer of RNase E the S1 domain forms a phosphate binding pocket. In Figure 31 the N terminal domains are represented as independent; however, the relative position of these domains in the three dimensional structure of RNase E is completely unknown. For example, the S1 domain may be in close proximity to the active site and therefore impart the enzyme's single -strand -specific activity. And it is also possible that the phosphate binding pocket lies within the catalytic domain of RNase E as suggested previously [2].

4.1.3 Structure and dimerization

The S1 domain of RNase E has been confirmed structurally as an S1 domain, a subclass of ob-fold domains. While this has been determined by sequence analysis previously, a high resolution structure is now available for aiding the determination of the function of this domain (Figure 7). The previous model of the S1 domain of RNase E was constructed by threading the RNase E sequence onto the PNPase S1 domain structure and has now been confirmed to be a reasonable estimate and a useful structure [61]. The general fold of the S1 domain predicted by Diwa et al. agrees with the NMR -derived and x-ray crystal structure. There are differences, however, the most obvious of which is the lack of secondary structure in the loop connecting β-sheet 3 and β-sheet 4 in the modelled domain (L3 in Figure 7).
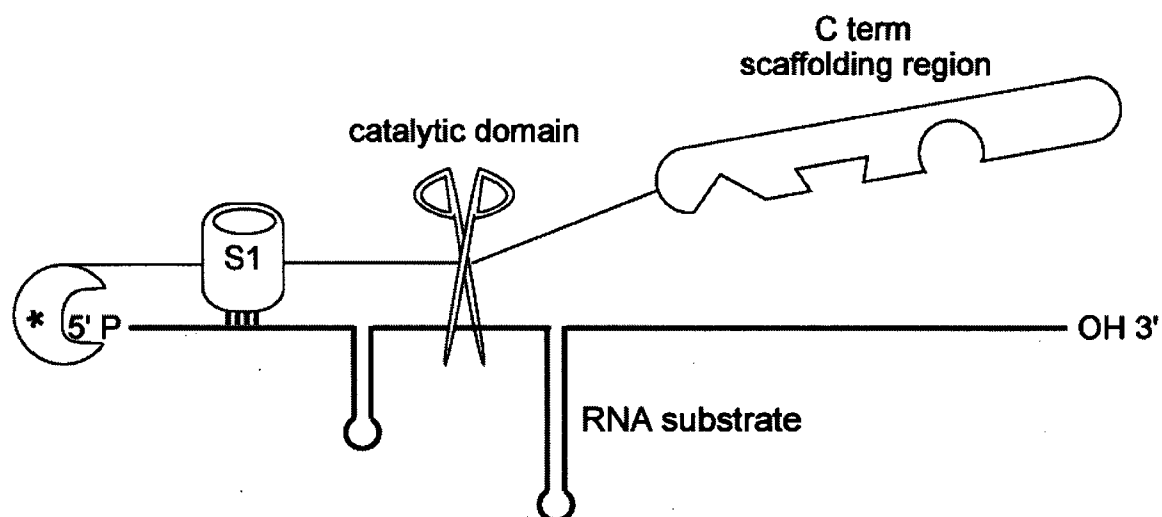
Figure 31: Domains in RNase E. A cartoon schematic of RNase E is shown with the amino terminus on the left and a substrate RNA molecule with the 5' end on the left. The S1 domain studied in this thesis is represented by a barrel binding substrate, the single -strand -specific catalytic domain is represented by the pair of scissors cutting the RNA substrate and the scaffolding region is represented as having binding sites for the components of the degradosome. The domain labelled * is the putative phosphate binding pocket. While this domain is represented at the extreme amino terminus, the location of this putative domain is unknown.

Multiple lines of evidence that the isolated S1 domain forms a dimer have been presented in this work. The NMR experimental work, conducted by Dr. Mario Schubert, indicates a concentration -dependent tumbling time that is longer than expected for a dimer. The tumbling time is consistent with an equilibrium between monomer and dimer. The tumbling time increases with increased S1 domain concentration, also consistent with an equilibrium in solution between monomer and dimer [95]. Additional NMR data contains intermolecular NOEs that are located on a putative dimerization surface distinct from the surface implicated in substrate binding. The high resolution x-ray crystal structure of the RNase E S1 domain (Figure 7), also the work of Dr. Mario Schubert, reveals an assymetric unit that contains two monomers. While not conclusive, this is also consistent with an ability of the domain to dimerize. Finally, glutaraldehyde crosslinking experiments show that the RNase E S1 domain can be crosslinked readily to form a larger species, likely a dimer (Figure 8).

The finding that the isolated RNase E S1 domain can form a dimer has consequences for the multimeric state of the full length enzyme. This is consistent with previous estimates of the stoichiometry of RNase E in the degradosome, which predict RNase E to exist as at least a dimer. This is also consistent with the quaternary structure of the highly homologous enzyme, RNase G, that suggest this endonuclease exists as a tetramer [100]. The finding of interacting amino acids in this domain that are separate from the RNA binding site suggest that this domain may have two functions within RNase E. The domain would serve to bind substrate and to provide for protein-protein contacts that stabilize an RNase E multimer. While the S1 domain may provide some contacts involved in stabilizing an RNase E multimer, it is clear that there must be others as the equilibrium in solution does not strongly favour a dimer (eg. Figure 8).

A model is presented in Figure 32 which attempts to account for the observed dimerization of the S1 domain of RNase E and recent evidence that RNase E is active as a tetramer [101]. The model predicts that the temperature -sensitive mutation G66S interrupts interactions in the RNase E tetramer as it does not appear to interrupt RNA binding or S1 domain dimerization.

4.1.4 RNA binding residues

The NMR titration data show a localized RNA interaction surface in the domain. This local surface is consistent with previous mutational studies of the RNase E S1 domain [61] and is the same region utilized by most ob-fold proteins to interact with nucleic acids [12]. Filter binding assays showing the importance of charge interactions in the recognition of nucleic acid by this domain were confirmed by the NMR titration experiment. The residues showing chemical shift perturbation included 3 lysines and 2 arginines (see figure 17). A large number of hydrophobic amino acids also showed alterations in chemical shift during the titration. These included a phenylalanine residue (F57) that in the homologous S1 domain of PNPase was predicted to bind RNA (see Figure 18) [58]. The three designed mutations in this study, F57A, R64A and R109A all showed defects in autoregulation *in vivo* in a previous study by Diwa et al. [61]. Diwa et al. went on to show that the RNase E catalytic domain (amino acids 1 – 601) containing F57A exhibited lower cleavage rates on model substrates *in vitro*. Surprisingly, although these mutants show defects *in vivo* and *in vitro*, the corresponding isolated S1 domain shows very little effect of these mutations on its affinity for RNA (Figure 19). It is possible that the RNA binding capacity of the domain is sufficiently different in the
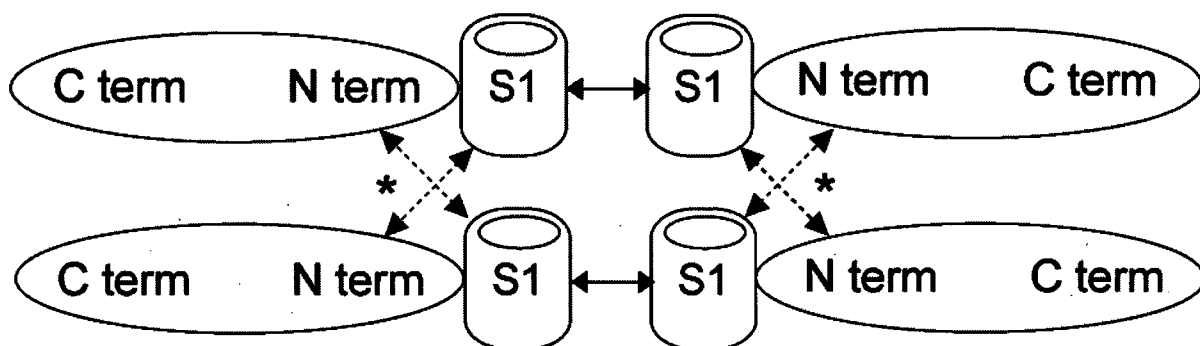
Figure 32: A model of RNase E multimerization. An RNase E tetramer is shown with each monomer containing an S1 domain represented by a barrel structure and the remaining carboxy terminus represented by an oval. The interactions uncovered in this work between S1 domains are indicated by solid double headed arrows. The model shows how a dimer of S1 domain may form in the context of an RNase E tetramer. The hypothesized interactions labelled * , indicated by dashed double headed arrows, may be involved in the dimerization of dimers of RNase E and may be disrupted by the *rne*-1 mutation leaving inactive RNase E monomers. The close coordination of S1 domains may also increase the affinity of RNase E for substrate.

context of the full length protein that these mutations become much more deleterious to RNA binding. It is also possible that the observed effects on autocontrol and *in vitro* catalysis of RNase E are not a function of the domain's ability to bind RNA, but reflect some other function of these residues (eg. dimerization).

4.1.5 *rne*-1 mutation

The structure of the S1 domain of RNase E as examined by CD revealed that the *rne-1* mutation disrupts the structure of the domain, as predicted by Diwa et al. [61]. The extent of this disruption was previously unknown. It is apparent that this mutation results in significant alteration of structure even at low temperatures (Figure 5). The effect of this temperature-sensitive mutation has been studied extensively [2]. Much like the engineered mutations, this mutation shows very little effect on RNA binding capacity as determined by the filter binding assay even at higher temperatures (see Figures 14 and 15). This points to another effect of this mutation in the context of the full length RNase E. It can be hypothesized that this mutation renders the domain unable to dimerize as effectively as the wild type. However, the *rne*-1 mutation in the S1 domain of RNase E does not prevent dimerization in the crosslinking experiment of Figure 8. The reason why this mutation eliminates catalytic activity from RNase E thus remains unknown.

Dimerization may be more favorable in the full length protein and this would decrease the K_d of the domain for RNA and alter other aspects of RNA binding. Thus, mutations with no obvious effect in the isolated domain would have an effect in the full length or catalytic domain of RNase E. Alternatively, these mutations may have an effect on the folding or stability of the full length RNase E that are not evident in the isolated domain.

Although problematic experimentally, the RNase contamination of the RNase E S1 domain preparations was interesting in itself. PNPase, which interacts with the distal C terminal end of full length RNase E is predicted to have different properties than the S1 domain of RNase E, yet persistently copurifies with this domain. Curiously an inverse form of interaction has been found between the S1 domain of PNPase the C terminal scaffolding region of RNase E (X. Miao, unpublished work). However, if the S1 domains of RNase E and PNPase do interact to promote copurification of PNPase and S1 domains, such an interaction can not be dectected by crosslinking (Figure 8 lanes 11 and 12).

Many possible avenues of investigation remain to clarify the role of the S1 domain in RNase E. Single alanine mutations in this domain may not exert much effect on its RNA binding properties. Thus, multiple mutations and/or mutations generating charge reversal might be more useful in determining important interacting residues. It is also possible that the engineered mutations made to date are not in residues that are important for RNA binding.

Determination of the structure of the *rne-1* RNase E S1 domain would be an interesting experiment if it can be performed. This may reveal structural features that are altered by this mutation and whether they lie in or near the RNA binding surface or closer to residues hypothesized to be involved in dimerization. Thus, allowing insight into which function of the domain is responsible for the severe phenotype of this mutation.

4.2 Function of PNPase S1 domain

This thesis has also investigated the properties of the S1 domain of PNPase and examined a long standing hypothesis that this domain imparts processive activity to the exonuclease [84, 85].

An important finding of the work examining PNPase is the altered activity of his-tagged PNPase as compared to wild type. While this difference was not examined in detail it is apparent that the different product and the lower activity of the N terminally tagged construct (Figure 22) is reason to abandon it as a model for endogenous PNPase.

My data show that the elimination of either the S1 domain or the KH domain of PNPase does not cause this enzyme to act distributively. It is possible that processivity is conferred by another site in PNPase or that the removal of one of the putative RNA binding domains is not sufficient to eliminate the processivity of PNPase.

RNase PH is highly homologous to PNPase, consisting of a hexamer of PH domains arranged around a central pore like PNPase [67]. However, RNase PH lacks the 'accessory' RNA binding motifs, the KH and S1 domains found in PNPase. However, Isii et al. have shown that RNase PH may be processive [102]. Their results do not prove the processivity of RNase PH with certainty since the assay in Figure 6 of their paper appears complete at the first time point.

Very interestingly, removing the S1 domain from PNPase blocks the ability of this enzyme to rescue the cold -sensitive phenotype of a PNPase null mutant (see Figure 26). This experiment was initially designed for three reasons. First, the PNPase S1 domain resembles cold shock domains [58]. Second, the cold-shock phenotype of a quadruple mutant of the Csp A family can be rescued by overexpressing the S1 domain

of PNPase [86]. Third PNPase expression is increased about 5-fold in cold shock and PNPase is, therefore, a cold-shock protein [72]. It is reasonable to hypothesize, therefore, that the S1 domain of PNPase plays a role during cold shock. The experiment in Figure 26 seems to confirm this possibility. However, the lower specific activity of the PNPase ΔS1 enzyme may account for its inability to rescue the *pnp* null mutant at low temperature. Expression of the constructs relies on leaky expression from the vector. Moreover, the constructs do not contain the 5' UTR and are not subject to autoregulation. Another interesting avenue would be to test PNPase ΔS1 phosphorolysis at lower temperatures to examine the possiblility that the S1 domain destabilizes secondary structures and enhances PNPase activity under these conditions.

Finally, the S1 domain of PNPase may play a direct role in the autocontrol of the enzyme. The S1 domain may recognize features of the 5' -UTR of the *pnp* transcript and facilitate its degradation. It is known that the KH and S1 domain are necessary for efficiency of the autoregulatory mechanism of PNPase [83].

Previous results from this laboratory indicate that the S1 domain of PNPase may be necessary for the interaction of PNPase with the degradsome (Miao, X., unpublished). This possibility suggests a dual function for the domain in protein-protein interaction and RNA binding. As seen with the S1 domain of RNase E, the S1 domain of PNPase contains protein interaction and RNA interaction surfaces.

The results of this thesis have shed light on the function of S1 domains in *E.coli* mRNA degradation. It is anticipated that many of the properties discovered in this work are also present in the S1 domains of the endoribonuclease RNase G and the

exoribonuclease RNase II. Many new questions about the S1 domain now have a basis from which to start.

5 Bibliography

1. Apirion, D., *Degradation of RNA in Escherichia coli. A hypothesis.* Mol Gen Genet, 1973. **122**(4): p. 313-22.

2. Coburn, G.A. and G.A. Mackie, *Degradation of mRNA in Escherichia coli: an old problem with some new twists.* Prog.Nucleic Acid Res.Mol.Biol., 1999. **62**: p. 55-108.

3. Deutscher, M.P. and N.B. Reuven, *Enzymatic basis for hydrolytic versus phosphorolytic mRNA degradation in Escherichia coli and Bacillus subtilis.* Proc Natl Acad Sci U S A, 1991. **88**(8): p. 3277-80.

4. Newbury, S.F., N.H. Smith, and C.F. Higgins, *Differential mRNA stability controls relative gene expression within a polycistronic operon.* Cell, 1987. **51**(6): p. 1131-43.

5. Masse, E., N. Majdalani, and S. Gottesman, *Regulatory roles for small RNAs in bacteria.* Curr Opin Microbiol, 2003. **6**(2): p. 120-4.

6. Carpousis, A.J., A. Leroy, N. Vanzo, and V. Khemici, *Escherichia coli RNA degradosome.* Methods Enzymol, 2001. **342**: p. 333-45.

7. Ghosh, S. and M.P. Deutscher, *Oligoribonuclease is an essential component of the mRNA decay pathway.* Proc Natl Acad Sci U S A, 1999. **96**(8): p. 4372-7.

8. Mackie, G.A., *Ribonuclease E is a 5'-end-dependent endonuclease.* Nature, 1998. **395**(6703): p. 720-723.

9. Carpousis, A.J., *The Escherichia coli RNA degradosome: structure, function and relationship in other ribonucleolytic multienzyme complexes.* Biochem Soc Trans, 2002. **30**(2): p. 150-5.

10. Coburn, G.A., X. Miao, D.J. Briant, and G.A. Mackie, *Reconstitution of a minimal RNA degradosome demonstrates functional coordination between a 3' exonuclease and a DEAD-box RNA helicase.* Genes Dev., 1999. **13**(19): p. 2594-2603.

11. Babitzke, P., L. Granger, J. Olszewski, and S.R. Kushner, *Analysis of mRNA decay and rRNA processing in Escherichia coli multiple mutants carrying a deletion in RNase III.* J Bacteriol, 1993. **175**(1): p. 229-39.

12. Theobald, D.L., R.M. Mitton-Fry, and D.S. Wuttke, *Nucleic acid recognition by OB-fold proteins.* Annu Rev Biophys Biomol Struct, 2003. **32**: p. 115-33.

13. Arcus, V., *OB-fold domains: a snapshot of the evolution of sequence, structure and function.* Curr Opin Struct Biol, 2002. **12**(6): p. 794-801.

14. Draper, D.E. and L.P. Reynaldo, *RNA binding strategies of ribosomal proteins.* Nucleic Acids Res, 1999. **27**(2): p. 381-8.

15. Murzin, A.G., *OB(oligonucleotide/oligosaccharide binding)-fold: common structural and functional solution for non-homologous sequences.* EMBO J, 1993. **12**(3): p. 861-7.

16. Schroder, K., P. Graumann, A. Schnuchel, T.A. Holak, and M.A. Marahiel, *Mutational analysis of the putative nucleic acid-binding surface of the cold-shock domain, CspB, revealed an essential role of aromatic and basic residues in binding of single-stranded DNA containing the Y-box motif.* Mol Microbiol, 1995. **16**(4): p. 699-708.

17. Kushner, S.R., *mRNA decay in Escherichia coli comes of age.* J Bacteriol, 2002. **184**(17): p. 4658-65; discussion 4657.

18. Kennell, D., *Processing endoribonucleases and mRNA degradation in bacteria*. J Bacteriol, 2002. **184**(17): p. 4645-57; discussion 4665.

19. Ghora, B.K. and D. Apirion, *Structural analysis and in vitro processing to p5 rRNA of a 9S RNA molecule isolated from an rne mutant of E. coli*. Cell, 1978. **15**(3): p. 1055-66.

20. Li, Z., S. Pandit, and M.P. Deutscher, *RNase G (CafA protein) and RNase E are both required for the 5' maturation of 16S ribosomal RNA*. EMBO J, 1999. **18**(10): p. 2878-85.

21. Lundberg, U. and S. Altman, *Processing of the precursor to the catalytic RNA subunit of RNase P from Escherichia coli*. RNA, 1995. **1**(3): p. 327-34.

22. Tomcsanyi, T. and D. Apirion, *Processing enzyme ribonuclease E specifically cleaves RNA I. An inhibitor of primer formation in plasmid DNA synthesis*. J Mol Biol, 1985. **185**(4): p. 713-20.

23. Lin-Chao, S. and S.N. Cohen, *The rate of processing and degradation of antisense RNAI regulates the replication of ColE1-type plasmids in vivo*. Cell, 1991. **65**(7): p. 1233-42.

24. Li, Z. and M.P. Deutscher, *RNase E plays an essential role in the maturation of Escherichia coli tRNA precursors*. RNA, 2002. **8**(1): p. 97-109.

25. Ow, M.C. and S.R. Kushner, *Initiation of tRNA maturation by RNase E is essential for cell viability in E. coli*. Genes Dev, 2002. **16**(9): p. 1102-15.

26. Ray, B.K. and D. Apirion, *Transfer RNA precursors are accumulated in Escherichia coli in the absence of RNase E*. Eur J Biochem, 1981. **114**(3): p. 517-24.

27.   Arraiano, C.M., S.D. Yancey, and S.R. Kushner, *Stabilization of discrete mRNA breakdown products in ams pnp rnb multiple mutants of Escherichia coli K-12.* J Bacteriol, 1988. **170**(10): p. 4625-33.

28.   Mackie, G.A., *Specific endonucleolytic cleavage of the mRNA for ribosomal protein S20 of Escherichia coli requires the product of the ams gene in vivo and in vitro.* J Bacteriol, 1991. **173**(8): p. 2488-97.

29.   Mackie, G.A., *Secondary structure of the mRNA for ribosomal protein S20. Implications for cleavage by ribonuclease E.* J Biol Chem, 1992. **267**(2): p. 1054-61.

30.   Baker, K.E. and G.A. Mackie, *Ectopic RNase E sites promote bypass of 5'-end-dependent mRNA decay in Escherichia coli.* Mol Microbiol, 2003. **47**(1): p. 75-88.

31.   Hajnsdorf, E., O. Steier, L. Coscoy, L. Teysset, and P. Regnier, *Roles of RNase E, RNase II and PNPase in the degradation of the rpsO transcripts of Escherichia coli: stabilizing function of RNase II and evidence for efficient degradation in an ams pnp rnb mutant.* EMBO J, 1994. **13**(14): p. 3368-77.

32.   Le Derout, J., M. Folichon, F. Briani, G. Deho, P. Regnier, and E. Hajnsdorf, *Hfq affects the length and the frequency of short oligo(A) tails at the 3' end of Escherichia coli rpsO mRNAs.* Nucleic Acids Res, 2003. **31**(14): p. 4017-23.

33.   Lopez, P.J., I. Marchand, S.A. Joyce, and M. Dreyfus, *The C-terminal half of RNase E, which organizes the Escherichia coli degradosome, participates in mRNA degradation but not rRNA processing in vivo.* Mol Microbiol, 1999. **33**(1): p. 188-99.

34.   Lin-Chao, S., T.T. Wong, K.J. McDowall, and S.N. Cohen, *Effects of nucleotide sequence on the specificity of rne-dependent and RNase E-mediated cleavages*

of RNA I encoded by the pBR322 plasmid. J Biol Chem, 1994. **269**(14): p. 10797-803.

35.   McDowall, K.J., V.R. Kaberdin, S.W. Wu, S.N. Cohen, and S. Lin-Chao, *Site-specific RNase E cleavage of oligonucleotides and inhibition by stem-loops.* Nature, 1995. **374**(6519): p. 287-90.

36.   Kaberdin, V.R., *Probing the substrate specificity of Escherichia coli RNase E using a novel oligonucleotide-based assay.* Nucleic Acids Res, 2003. **31**(16): p. 4710-6.

37.   Steitz, T.A. and J.A. Steitz, *A general two-metal-ion mechanism for catalytic RNA.* Proc Natl Acad Sci U S A, 1993. **90**(14): p. 6498-502.

38.   Misra, T.K. and D. Apirion, *RNase E, an RNA processing enzyme from Escherichia coli.* J Biol Chem, 1979. **254**(21): p. 11154-9.

39.   Cohen, S.N. and K.J. McDowall, *RNase E: still a wonderfully mysterious enzyme.* Mol Microbiol, 1997. **23**(6): p. 1099-106.

40.   McDowall, K.J. and S.N. Cohen, *The N-terminal domain of the rne gene product has RNase E activity and is non-overlapping with the arginine-rich RNA-binding site.* J Mol Biol, 1996. **255**(3): p. 349-55.

41.   Cormack, R.S., J.L. Genereaux, and G.A. Mackie, *RNase E activity is conferred by a single polypeptide: overexpression, purification, and properties of the ams/rne/hmp1 gene product.* Proc Natl Acad Sci U S A, 1993. **90**(19): p. 9006-10.

42.   Taraseviciene, L., G.R. Bjork, and B.E. Uhlin, *Evidence for an RNA binding region in the Escherichia coli processing endoribonuclease RNase E.* J Biol Chem, 1995. **270**(44): p. 26391-8.

43.   Burd, C.G. and G. Dreyfuss, *Conserved structures and diversity of functions of RNA-binding proteins.* Science, 1994. **265**(5172): p. 615-21.

44.   Kaberdin, V.R., Y.H. Chao, and S. Lin-Chao, *RNase E cleaves at multiple sites in bubble regions of RNA I stem loops yielding products that dissociate differentially from the enzyme.* J Biol Chem, 1996. **271**(22): p. 13103-9.

45.   Diwa, A., A.L. Bricker, C. Jain, and J.G. Belasco, *An evolutionarily conserved RNA stem-loop functions as a sensor that directs feedback regulation of RNase E gene expression.* Genes Dev, 2000. **14**(10): p. 1249-60.

46.   Carpousis, A.J., G. Van Houwe, C. Ehretsmann, and H.M. Krisch, *Copurification of E. coli RNAase E and PNPase: evidence for a specific association between two enzymes important in RNA processing and degradation.* Cell, 1994. **76**(5): p. 889-900.

47.   Vanzo, N.F., Y.S. Li, B. Py, E. Blum, C.F. Higgins, L.C. Raynal, H.M. Krisch, and A.J. Carpousis, *Ribonuclease E organizes the protein interactions in the Escherichia coli RNA degradosome.* Genes Dev, 1998. **12**(17): p. 2770-81.

48.   Py, B., C.F. Higgins, H.M. Krisch, and A.J. Carpousis, *A DEAD-box RNA helicase in the Escherichia coli RNA degradosome.* Nature, 1996. **381**(6578): p. 169-72.

49.   Miczak, A., V.R. Kaberdin, C.L. Wei, and S. Lin-Chao, *Proteins associated with RNase E in a multicomponent ribonucleolytic complex.* Proc Natl Acad Sci U S A, 1996. **93**(9): p. 3865-9.

50.   Kido, M., K. Yamanaka, T. Mitani, H. Niki, T. Ogura, and S. Hiraga, *RNase E polypeptides lacking a carboxyl-terminal half suppress a mukB mutation in Escherichia coli.* J Bacteriol, 1996. **178**(13): p. 3917-25.

51. Lee, K. and S.N. Cohen, *A Streptomyces coelicolor functional orthologue of Escherichia coli RNase E shows shuffling of catalytic and PNPase-binding domains.* Mol Microbiol, 2003. **48**(2): p. 349-60.

52. Leroy, A., N.F. Vanzo, S. Sousa, M. Dreyfus, and A.J. Carpousis, *Function in Escherichia coli of the non-catalytic part of RNase E: role in the degradation of ribosome-free mRNA.* Mol Microbiol, 2002. **45**(5): p. 1231-43.

53. Jain, C. and J.G. Belasco, *RNase E autoregulates its synthesis by controlling the degradation rate of its own mRNA in Escherichia coli: unusual sensitivity of the rne transcript to RNase E activity.* Genes Dev, 1995. **9**(1): p. 84-96.

54. Diwa, A.A. and J.G. Belasco, *Critical features of a conserved RNA stem-loop important for feedback regulation of RNase E synthesis.* J Biol Chem, 2002. **277**(23): p. 20415-22.

55. Mohanty, B.K. and S.R. Kushner, *Polyadenylation of Escherichia coli transcripts plays an integral role in regulating intracellular levels of polynucleotide phosphorylase and RNase E.* Mol Microbiol, 2002. **45**(5): p. 1315-24.

56. Jiang, X., A. Diwa, and J.G. Belasco, *Regions of RNase E important for 5'-end-dependent RNA cleavage and autoregulated synthesis.* J Bacteriol, 2000. **182**(9): p. 2468-75.

57. Ow, M.C., Q. Liu, and S.R. Kushner, *Analysis of mRNA decay and rRNA processing in Escherichia coli in the absence of RNase E-based degradosome assembly.* Mol Microbiol, 2000. **38**(4): p. 854-66.

58. Bycroft, M., T.J. Hubbard, M. Proctor, S.M. Freund, and A.G. Murzin, *The solution structure of the S1 RNA binding domain: a member of an ancient nucleic acid-binding fold.* Cell, 1997. **88**(2): p. 235-242.

59. Babitzke, P. and S.R. Kushner, *The Ams (altered mRNA stability) protein and ribonuclease E are encoded by the same structural gene of Escherichia coli.* Proc Natl Acad Sci U S A, 1991. **88**(1): p. 1-5.

60. Misra, T.K. and D. Apirion, *Gene rne affects the structure of the ribonucleic acid-processing enzyme ribonuclease E of Escherichia coli.* J Bacteriol, 1980. **142**(1): p. 359-61.

61. Diwa, A.A., X. Jiang, M. Schapira, and J.G. Belasco, *Two distinct regions on the surface of an RNA-binding domain are crucial for RNase E function.* Mol Microbiol, 2002. **46**(4): p. 959-69.

62. Portier, C., *Isolation of a polynucleotide phosphorylase mutant using a kanamycin resistant determinant.* Mol Gen Genet, 1980. **178**(2): p. 343-9.

63. Portier, C., *Quaternary structure of Escherichia coli polynucleotide phosphorylase: new evidence for a trimeric structure.* FEBS Lett, 1975. **50**(1): p. 79-81.

64. Grunberg-Manago, M., *Recollections on studies of polynucleotide phosphorylase: a commentary on 'Enzymic Synthesis of Polynucleotides. I. Polynucleotide Phosphorylase of Azobacter vinelandii'.* Biochim.Biophys.Acta, 1989. **1000**: p. 59-64.

65. Gillam, S. and M. Smith, *Use of E. coli polynucleotide phosphorylase for the synthesis of oligodeoxyribonucleotides of defined sequence.* Methods Enzymol, 1980. **65**(1): p. 687-701.

66. Zhou, Z. and M.P. Deutscher, *An essential function for the phosphate-dependent exoribonucleases RNase PH and polynucleotide phosphorylase.* J.Bacteriol., 1997. **179**(13): p. 4391-4395.

67. Symmons, M.F., G.H. Jones, and B.F. Luisi, *A duplicated fold is the structural basis for polynucleotide phosphorylase catalytic activity, processivity, and regulation.* Structure.Fold.Des, 2000. **8**(11): p. 1215-1226.

68. Donovan, W.P. and S.R. Kushner, *Polynucleotide phosphorylase and ribonuclease II are required for cell viability and mRNA turnover in Escherichia coli K-12.* Proc Natl Acad Sci U S A, 1986. **83**(1): p. 120-4.

69. Blum, E., A.J. Carpousis, and C.F. Higgins, *Polyadenylation promotes degradation of 3'-structured RNA by the Escherichia coli mRNA degradosome in vitro.* J Biol Chem, 1999. **274**(7): p. 4009-16.

70. Xu, F. and S.N. Cohen, *RNA degradation in Escherichia coli regulated by 3' adenylation and 5' phosphorylation.* Nature, 1995. **374**(6518): p. 180-3.

71. McLaren, R.S., S.F. Newbury, G.S. Dance, H.C. Causton, and C.F. Higgins, *mRNA degradation by processive 3'-5' exoribonucleases in vitro and the implications for prokaryotic mRNA decay in vivo.* J Mol Biol, 1991. **221**(1): p. 81-95.

72. Polissi, A., W. De Laurentis, S. Zangrossi, F. Briani, V. Longhi, G. Pesole, and G. Deho, *Changes in Escherichia coli transcriptome during acclimatization at low temperature.* Res Microbiol, 2003. **154**(8): p. 573-80.

73. Yamanaka, K. and M. Inouye, *Selective mRNA degradation by polynucleotide phosphorylase in cold shock adaptation in Escherichia coli.* J Bacteriol, 2001. **183**(9): p. 2808-16.

74. Beran, R.K. and R.W. Simons, *Cold-temperature induction of Escherichia coli polynucleotide phosphorylase occurs by reversal of its autoregulation.* Mol Microbiol, 2001. **39**(1): p. 112-25.

75. Jarrige, A.C., N. Mathy, and C. Portier, *PNPase autocontrols its expression by degrading a double-stranded structure in the pnp mRNA leader.* EMBO J, 2001. **20**(23): p. 6845-55.

76. Yehudai-Resheff, S., V. Portnoy, S. Yogev, N. Adir, and G. Schuster, *Domain analysis of the chloroplast polynucleotide phosphorylase reveals discrete functions in RNA degradation, polyadenylation, and sequence homology with exosome proteins.* Plant Cell, 2003. **15**(9): p. 2003-19.

77. Symmons, M.F., G.H. Jones, and B.F. Luisi, *A duplicated fold is the structural basis for polynucleotide phosphorylase catalytic activity, processivity, and regulation.* Structure Fold Des, 2000. **8**(11): p. 1215-26.

78. Musco, G., G. Stier, C. Joseph, M.A. Castiglione Morelli, M. Nilges, T.J. Gibson, and A. Pastore, *Three-dimensional structure and stability of the KH domain: molecular insights into the fragile X syndrome.* Cell, 1996. **85**(2): p. 237-45.

79. Leffers, H., K. Dejgaard, and J.E. Celis, *Characterisation of two major cellular poly(rC)-binding human proteins, each containing three K-homologous (KH) domains.* Eur J Biochem, 1995. **230**(2): p. 447-53.

80. Urlaub, H., V. Kruft, O. Bischof, E.C. Muller, and B. Wittmann-Liebold, *Protein-rRNA binding features and their structural and functional implications in ribosomes as determined by cross-linking studies.* EMBO J, 1995. **14**(18): p. 4578-88.

81. Liu, K. and M.M. Hanna, *NusA contacts nascent RNA in Escherichia coli transcription complexes.* J Mol Biol, 1995. **247**(4): p. 547-58.

82. Lewis, H.A., K. Musunuru, K.B. Jensen, C. Edo, H. Chen, R.B. Darnell, and S.K. Burley, *Sequence-specific RNA binding by a Nova KH domain: implications for*

paraneoplastic disease and the fragile X syndrome. Cell, 2000. **100**(3): p. 323-32.

83.   Jarrige, A., D. Brechemier-Baey, N. Mathy, O. Duche, and C. Portier, *Mutational analysis of polynucleotide phosphorylase from Escherichia coli.* J Mol Biol, 2002. **321**(3): p. 397-409.

84.   Godefroy, T., *Kinetics of polymerization and phosphorolysis reactions of Escherichia coli polynucleotide phosphorylase. Evidence for multiple binding of polynucleotide in phosphorolysis.* Eur J Biochem, 1970. **14**(2): p. 222-31.

85.   Symmons, M.F., M.G. Williams, B.F. Luisi, G.H. Jones, and A.J. Carpousis, *Running rings around RNA: a superfamily of phosphate-dependent RNases.* Trends Biochem Sci, 2002. **27**(1): p. 11-8.

86.   Xia, B., H. Ke, and M. Inouye, *Acquirement of cold sensitivity by quadruple deletion of the cspA family and its suppression by PNPase S1 domain in Escherichia coli.* Mol Microbiol, 2001. **40**(1): p. 179-88.

87.   Newkirk, K., W. Feng, W. Jiang, R. Tejero, S.D. Emerson, M. Inouye, and G.T. Montelione, *Solution NMR structure of the major cold shock protein (CspA) from Escherichia coli: identification of a binding epitope for DNA.* Proc Natl Acad Sci U S A, 1994. **91**(11): p. 5114-8.

88.   Schindelin, H., W. Jiang, M. Inouye, and U. Heinemann, *Crystal structure of CspA, the major cold shock protein of Escherichia coli.* Proc Natl Acad Sci U S A, 1994. **91**(11): p. 5119-23.

89.   Bae, W., B. Xia, M. Inouye, and K. Severinov, *Escherichia coli CspA-family RNA chaperones are transcription antiterminators.* Proc Natl Acad Sci U S A, 2000. **97**(14): p. 7784-9.

90. Mullis, K., F. Faloona, S. Scharf, R. Saiki, G. Horn, and H. Erlich, *Specific enzymatic amplification of DNA in vitro: the polymerase chain reaction.* Cold Spring Harb Symp Quant Biol, 1986. **51 Pt 1**: p. 263-73.

91. Coburn, G.A. and G.A. Mackie, *Reconstitution of the degradation of the mRNA for ribosomal protein S20 with purified enzymes.* J.Mol.Biol., 1998. **279**(5): p. 1061-1074.

92. Spickler, C. and G.A. Mackie, *Action of RNase II and polynucleotide phosphorylase against RNAs containing stem-loops of defined structure.* J.Bacteriol., 2000. **182**(9): p. 2422-2427.

93. Cormack, R.S. and G.A. Mackie, *Structural requirements for the processing of Escherichia coli 5 S ribosomal RNA by RNase E in vitro.* J Mol Biol, 1992. **228**(4): p. 1078-90.

94. Wong, I. and T.M. Lohman, *A double-filter method for nitrocellulose-filter binding: application to protein-nucleic acid interactions.* Proc Natl Acad Sci U S A, 1993. **90**(12): p. 5428-32.

95. Gryk, M.R., R. Abseher, B. Simon, M. Nilges, and H. Oschkinat, *Heteronuclear relaxation study of the PH domain of beta-spectrin: restriction of loop motions upon binding inositol trisphosphate.* J Mol Biol, 1998. **280**(5): p. 879-96.

96. Causton, H., B. Py, R.S. McLaren, and C.F. Higgins, *mRNA degradation in Escherichia coli: a novel factor which impedes the exoribonucleolytic activity of PNPase at stem-loop structures.* Mol Microbiol, 1994. **14**(4): p. 731-41.

97. Phadtare, S. and M. Inouye, *Sequence-selective interactions with RNA by CspB, CspC and CspE, members of the CspA family of Escherichia coli.* Mol Microbiol, 1999. **33**(5): p. 1004-14.

98. Jiang, W., Y. Hou, and M. Inouye, *CspA, the major cold-shock protein of Escherichia coli, is an RNA chaperone.* J Biol Chem, 1997. **272**(1): p. 196-202.

99. Spickler, C., V. Stronge, and G.A. Mackie, *Preferential cleavage of degradative intermediates of rpsT mRNA by the Escherichia coli RNA degradosome.* J.Bacteriol., 2001. **183**(3): p. 1106-1109.

100. Briant, D.J., J.S. Hankins, M.A. Cook, and G.A. Mackie, *The quaternary structure of RNase G from Escherichia coli.* Mol Microbiol, 2003. **50**(4): p. 1381-90.

101. Callaghan, A.J., J.G. Grossmann, Y.U. Redko, L.L. Ilag, M.C. Moncrieffe, M.F. Symmons, C.V. Robinson, K.J. McDowall, and B.F. Luisi, *Quaternary Structure and Catalytic Activity of the Escherichia coli Ribonuclease E Amino-Terminal Catalytic Domain.* Biochemistry, 2003. **42**(47): p. 13848-13855.

102. Ishii, R., O. Nureki, and S. Yokoyama, *Crystal structure of the tRNA processing enzyme RNase PH from Aquifex aeolicus.* J Biol Chem, 2003. **278**(34): p. 32397-404.